SPECIAL REINFORCED MASONRY RIGID-WALL FLEXIBLE-DIAPHRAGM FUNCTIONAL RECOVERY PREQUALIFICATION

Final Report Submitted to the PUC (1/5/2026) for Consideration in the 2026 NEHRP Provisions

RESILIENT DESIGN FOR FUNCTIONAL RECOVERY: PREQUALIFICATION REPORT FOR SPECIAL REINFORCED MASONRY RIGID-WALL FLEXIBLE-DIAPHRAGM SYSTEMS

Final Report Submitted to the PUC for Consideration in the 2026 NEHRP Provisions

Prepared By:

Resilient Design Coalition

Financially Supported by:

Concrete Masonry & Hardscapes Association, Concrete Masonry Checkoff, and the Charles Pankow Foundation

WORKING GROUP MEMBERS:

Ed Almeter, MS
Kristen Blowes, PhD, PE
Jared DeBock, PhD, PE
Curt Haselton, PhD, PE
Carlos Molina Hutt, PhD, PE
Huy Pham, PhD
David Welch, PhD
Reid Zimmerman, SE

January 5, 2026

QUANTIFICATION OF FUNCTIONAL RECOVERY SEISMIC PERFORMANCE FACTORS FOR THE SPECIAL REINFORCED MASONRY RIGID WALL FLEXIBLE DIAPHRAGM SYSTEM

Submitted: 1/5/2026

EXECUTIVE SUMMARY

This report documents the quantification of the functional recovery seismic performance factors for the one-story special reinforced masonry rigid wall flexible diaphragm (RM-RWFD) system. All buildings assessed in this study conform to the limitations outlined in Section 12.10.4.1 of ASCE/SEI 7-22 with perimeter vertical load resisting elements that place a substantial load on the out-of-plane diaphragm connections. Quantification of the functional recovery seismic performance factors is performed in accordance with the proposed Section A.8 procedures of the 2026 National Earthquake Hazards Reduction Program (NEHRP) Provisions. The functional recovery seismic performance factors for RWFD systems include the functional recovery response modification coefficient, R_{fr}, the functional recovery allowable story drift limit, $\Delta_{afr.}$, and the functional recovery structure ductility reduction factor, $R_{\mu fr}$, along with three additional parameters: $R_{diaph,fr}$ is the response modification coefficient for diaphragm design, $\Delta_{a,diaph,fr}$ is the functional recovery allowable diaphragm story drift limit, and $I_{pfr,oop}$ is the component importance factor used for out-of-plane design forces for walls and wall anchorage.

The functional recovery seismic performance factors were determined by developing an archetype space of different building configurations, designed with various $R_{diaph,fr}$ and $I_{pfr,oop}$, and then selecting the combination that results in less than a 10% mean probability of Safety-Critical Structural Damage, or P[SCSD], in each performance group, and less than 20% P[SCSD] for any individual archetype, for Functional Recovery Category (FRC) A, B and C. The 10% and 20% thresholds are modified to 15% and 25%, respectively, for FRC D. Additional checks are performed to ensure variations in R_{fr}, Δ_{afr}, $\Delta_{a,diaphr,fr}$, and $R_{\mu fr}$ satisfy the prescribed acceptance criteria.

The required values of $R_{diaph,fr}$ and $\Delta_{a.diaph,fr}$ based on analysis are compared to the judgment-based limits according to Appendix A of NEHRP 2026, and the more stringent values are selected. The judgment-based limits of $R_{diaph,fr}$ are $R_{diaph}/1.5$ and $R_{diaph}/1.25$ for FRC A/B/C and FRC D, respectively, with R_{diaph} as specified in ASCE/SEI 7-22 Section 12.10.4.2.1. The judgment-based limits of $\Delta_{a,diaph,fr}$ are 1.25% and 1.75% for FRC A/B/C and FRC D, respectively. System specific $R_{\mu fr}$ factors are determined by comparing peak floor acceleration demands from the analysis with the seismic floor accelerations from Section A.10.6 in accordance with Section A.8.3.6 procedures in Appendix A of the 2026 NEHRP Provisions. Verification of R_{fr} and Δ_{afr} for in-plane masonry wall response is carried out in a separate study.

All analyses are conducted at the Functional Recovery Earthquake (FRE_R) level shaking corresponding to a Seismic Design Category $D_{max,FRE}$ condition with two-point spectral ordinates

S_{dsfr} and S_{d1fr} of 1.25 and 0.75, respectively. The standard Equivalent Lateral Force (ELF) procedure outlined in ASCE 7-22 (ASCE, 2022) Sections 12.10.1 and 12.10.2 for diaphragms, chords, and collectors is used for design in the current study. The proposed functional recovery seismic performance factors are also checked for compliance against the SCSD acceptance criteria using the alternative diaphragm design provisions of ASCE 7-22 Section 12.10.4. The application of the ASCE 7-22 Section 12.10.3 alternative diaphragm design provisions to the archetypes and the resulting seismic provisions was not considered in this study.

The proposed $R_{diaph,fr}$, $\Delta_{a,diaph,fr}$, $I_{pfr,oop}$, R_{fr}, Δ_{afr}, and $R_{\mu fr}$ for RM-RWFD are presented in the tables below. For RM-RWFD buildings, peak story drifts include both the in-plane wall displacement amplified by $C_{d\text{-}fr}$ (where $C_{d\text{-}fr}$ is equal to R_{fr}) and diaphragm displacements amplified by $C_{d\text{-}diaph,fr}$ (where $C_{d\text{-}diaph,fr}$ is equal to $R_{diaph,fr}$). The proposed seismic parameters for $R_{fr,}$ and Δ_{afr} are specific to special reinforced masonry RWFD buildings, per the RDC prequalification report for special reinforced masonry shear wall systems. $R_{diaph,fr}$, $\Delta_{a,diaph,fr}$, $I_{pfr,oop}$, and $R_{\mu fr}$ are generally applicable for other RWFD systems satisfying the limitations of ASCE/SEI 7-22 Section 12.10.4.1.

Table 1 – Proposed design criteria to satisfy the Functional Recovery Category A/B/C performance objectives for RM-RWFD systems

System	FRC A/B/C					
	$R_{diaph,fr}$	$\Delta_{a,diaph,fr}$	$I_{pfr,oop}$	$R_{\mu fr}$	R_{fr}*	Δ_{afr}*
Wood Diaphragm†	3.0	1.25%	1.5	1.3	2.5, 3.5**	0.5%
Bare Steel Deck Diaphragm‡	3.0	1.25%	1.5	1.3	2.5, 3.5**	0.5%

† Design and detailing according to AWC SDPWS Section 4.2 for blocked diaphragms. Limited to one story buildings.
‡ Diaphragm detailing conforms to the special seismic detailing defined in AISI S400 Section F3. Limited to one story buildings.
* Values of R_{fr} and Δ_{afr} are from the RDC prequalification report on special reinforced masonry shear wall systems.
** R_{fr} is 2.5 for buildings with shear-controlled wall segments and 3.5 for buildings with all flexure-controlled wall segments in a given direction.

Table 2 – Proposed design criteria to satisfy the Functional Recovery Category D performance objectives for RM-RWFD systems

System	FRC D					
	$R_{diaph,fr}$	$\Delta_{a,diaph,fr}$	$I_{pfr,oop}$	$R_{\mu fr}$	R_{fr}*	Δ_{afr}*
Wood Diaphragm†	3.5	1.75%	1.25	1.35	3.0, 4.0**	0.5%
Bare Steel Deck Diaphragm‡	3.5	1.75%	1.25	1.35	3.0, 4.0**	0.5%

† Design and detailing according to AWC SDPWS Section 4.2 for blocked diaphragms. Limited to one story buildings.
‡ Diaphragm detailing conforms to the special seismic detailing defined in AISI S400 Section F3. Limited to one story buildings.
* Values of R_{fr} and Δ_{afr} are from the RDC prequalification report on special reinforced masonry shear wall systems.
** R_{fr} is 3.0 for buildings with shear-controlled wall segments and 4.0 for buildings with all flexure-controlled wall segments in a given direction.

Contents

Executive Summary 1
1. Introduction 5
1.1. System Overview 6
1.2. Code Considerations for RWFD Structures 9
1.2.1. Adopted Design Approach for Diaphragm Design 9
1.2.2. Recent Evolution of the Flexible Steel Diaphragm Design 10
2. Analysis Methods 11
2.1. Design Iteration and Acceptance Criteria for Seismic Performance Factors 11
2.1.1. Safety-Critical Structural Damage (SCSD) 12
2.1.2. System Specific SCSD Considerations 12
2.2. Fragility Functions for the RM-RWFD System 12
2.2.1. Wood Roof Diaphragm Fragilities 13
2.2.2. Out-of-Plane Wall-to-Diaphragm Anchorage Fragilities 18
2.2.3. Out-of-Plane Wall Fragilities 21
2.3. Archetypes Considered for Analysis 24
2.3.1. Building Configuration and Structural Component Population 24
2.3.2. Performance Groups for RM-RWFD Systems 26
2.4. Estimation of Structural Responses 27
2.4.1. Analytical Basis Behind the RWFD Structural Response Prediction Engine (SRPE) 27
2.4.2. Structural Properties Estimation 30
2.4.3. Summary of EDP's predicted by the RWFD SRPE 32
3. Results 33
3.1. FRC A/B/C Analysis Results 34
3.2. FRC D Analysis Results 34
3.3. System Response 35
3.4. Validation of Peak Floor Acceleration Demand Estimates 36
4. Conclusions and Recommendations 37

4.1. Design Strength Requirements for Wood Diaphragms in Masonry RWFD Buildings. 37

4.2. Design Strength Requirements for Other Types of Diaphragms in Masonry RWFD Buildings 38

4.3. Design Strength Requirements for the Masonry Walls In-Plane 38

4.4. Design Strength Requirements for the Masonry Walls Out-of-Plane 39

4.5. Use of the Various ASCE 7 Design Methods for RWFD Buildings 39

Supplementary Material 40

References 41

1. INTRODUCTION

This report documents the quantification of the functional recovery seismic performance factors for the special reinforced masonry rigid wall flexible diaphragm (RM-RWFD) system. Quantification of the functional recovery seismic performance factors is performed in accordance with the proposed Section A.8 procedures of the 2026 National Earthquake Hazards Reduction Program (NEHRP) Provisions. The functional recovery seismic performance factors include the functional recovery response modification coefficient, $R_{fr,}$ the functional recovery allowable story drift limit, Δ_{afr}, and the functional recovery structure ductility reduction factor, $R_{\mu fr.}$ These are the equivalents of the response modification coefficient, R, the allowable story drift limit, Δ_a, and the structure ductility reduction factor, R_μ, used in ASCE/SEI 7 Chapters 12 and 13, but for design for functional recovery. For this system there are three additional parameters: $R_{diaph,fr}$ is the response modification coefficient for diaphragm design, $\Delta_{a,diaph,fr}$ is the functional recovery allowable diaphragm story drift limit, and $I_{p,fr,oop}$ is the component importance factor used for out-of-plane design forces for walls and wall anchorage. The scope of the functional recovery seismic performance factor assessment performed herein is limited to one-story RM-RWFD structures, complying with the limitations outlined in Section 12.10.4.1 of ASCE/SEI 7-22.

An archetype space of different wall heights and plan configurations, designed with various functional recovery response modification coefficients was developed. FEMA P-58/ATC-138 (FEMA, 2018a; ATC, 2021) models were then created. In accordance with the proposed Section A.8 procedures of the 2026 NEHRP Provisions, only structural components are included in these FEMA P-58/ATC-138 performance models. Design of the archetypes was performed using the automated design capability of SP3 (www.sp3risk.com) and engineering demand parameters (e.g., story drift ratios, diaphragm ductility demand, out-of-plane wall drift, wall anchorage forces, etc.) were estimated using SP3's Response Prediction Engine, which while calibrated based on extensive nonlinear response history analyses, does not perform nonlinear response history analyses of the specific archetype directly.

Performance assessments of each model are conducted in accordance with FEMA P-58 (FEMA, 2018a) and ATC-138 recommendations to quantify the probability of safety-critical structural damage (P[SCSD]) for each archetype (Blowes et al., in press). The assigned safety class governs the triggering of SCSD for a given component and damage state according to the ATC-138 methodology. The safety class controls what percentage of components, in each story and direction, that can be in each damage state or greater, prior to triggering SCSD in the building. The P[SCSD] serves as an acceptable proxy for the probability of exceeding the target functional recovery times for structural-only models, as outlined in section CA.8.3.5 of the 2026 NEHRP Seismic Provisions.

The functional recovery seismic performance factors are selected such that archetypes designed for that $R_{diaph,fr}$ and $I_{p,fr,oop}$ result in less than a 10% mean P[SCSD] in each performance group and less than 20% P[SCSD] for any individual archetype for Functional Recovery Category (FRC) A, B and C. The 10% and 20% are modified to 15% and 25%, respectively, for FRC D. Additional checks are performed to ensure variations in R_{fr}, Δ_{afr}, $\Delta_{a,diaphr,fr}$, and, $R_{\mu fr}$ satisfy the prescribed acceptance criteria and do not create undue demands for non-structural components. All analyses are conducted at the Functional Recovery Earthquake (FRE_R) level shaking corresponding to a Seismic Design Category $D_{max,FRE}$ condition with two-point spectral ordinates S_{dsfr} and S_{d1fr} of 1.25 and 0.75, respectively.

1.1. System Overview

RWFD structures are typically one-story structures with large roof diaphragm spans between lateral force resisting members. Diaphragms are commonly constructed of either wood or bare steel deck as a covering material, as shown in Figure 1.

Figure 1. Example aerial views of rigid wall flexible diaphragm structures: a) wood roof diaphragm; b) bare steel deck diaphragm (Images adapted from FEMA, 2021)

Modern wood diaphragm systems commonly consist of panelized wood structural panels (e.g., plywood or OSB) fastened to wood subpurlins (i.e., nailers) that frame into a wood or steel joist system for primary framing, with the combination of wood and steel framing termed a "hybrid system" (Lawson, 2008; 2013). Sheathing to framing connections are typically common nails, where the thickness of the framing members varies (e.g., 2X, 3X or 4X dimensional lumber) depending on the nail size and spacing requirements for the field and edges of panels (AWC, 2021). Example details of a wood diaphragm system for RWFD buildings are shown in Figure 2.

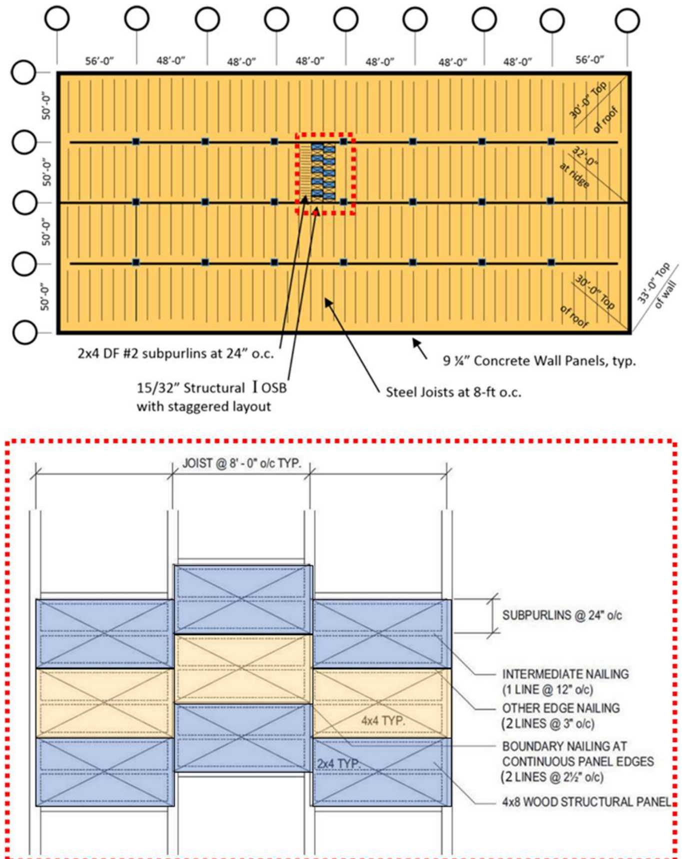

Figure 2. Main components of a modern wood diaphragm system: primary framing (above), local sheathing and framing details (below). Images adapted from Wade et al. (2018) and Lawson (2013).

Bare steel deck diaphragm systems use flexible cold-formed steel decking that is supported by a system of open steel truss elements (i.e., subpurlins and girders) that transfer vertical loads to exterior walls and interior gravity columns. An example of a bare steel deck diaphragm system is shown in Figure 3. In order to provide diaphragm action, bare steel deck systems require structural connections at the point of contact with the steel framing as well as connections at the sides of adjacent panels (i.e., side-laps). Structural connections can be welds (e.g., arc spot welds) or mechanical fasteners (e.g., PAFs). Similarly, side-lap connections can be welded (e.g., seam welds) or mechanical (e.g., screws or button punches). The applicability of different side-lap connections depends on the decking system used, where the side-lap could be nested or interlocking, as shown in Figure 4 (SDI, 2015). Side-lap connections provide shear strength to the diaphragm, while structural connections allow for force redistribution. Due to the numerous possible combinations of steel panel connections, the expected strength and ductility capacity of bare steel deck diaphragms can vary considerably. This is reflected in the recent updates to ASCE 41/AISC 342 (ASCE, 2023; AISC, 2022) documents for bare steel deck diaphragms based on recent experimental and analytical studies (Schafer, 2019; Wei et al. 2019).

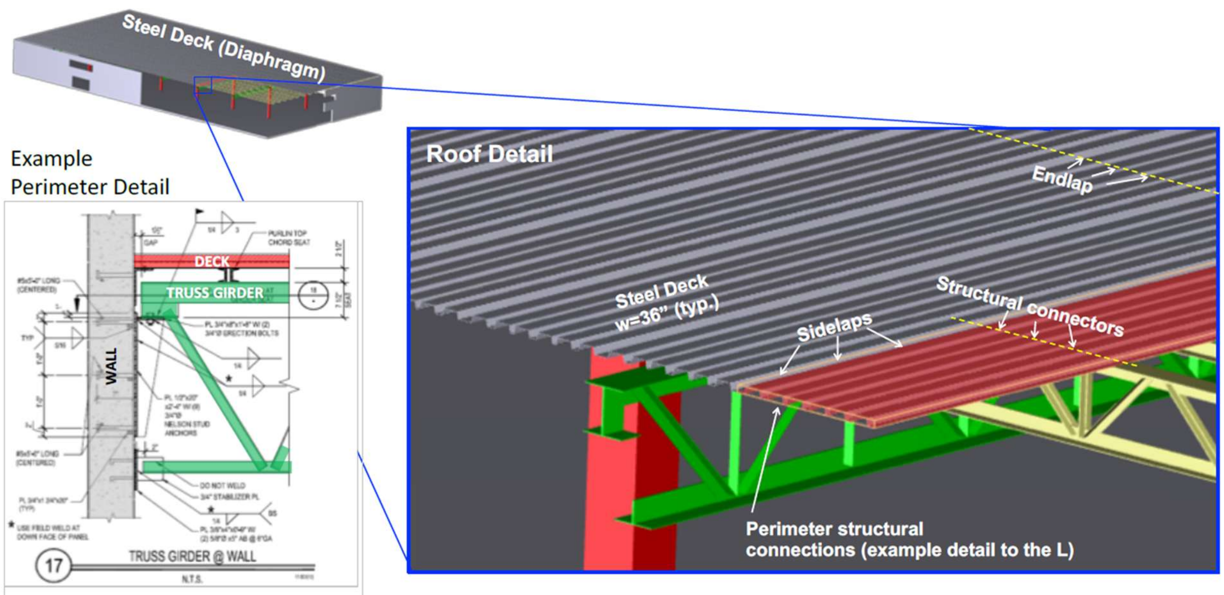

Figure 3. Main components of a modern bare steel deck diaphragm system (Schafer, 2018; 2019).

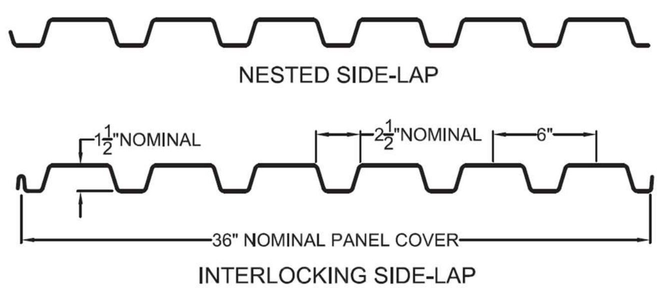

Figure 4. Different side-lap conditions for steel deck panels (SDI, 2015; FEMA, 2021).

The RWFD term is attributed to these structures due to the large difference in lateral stiffness between vertical lateral force resisting elements (i.e., walls) and the roof diaphragm. When subjected to seismic loading, the diaphragm is expected to experience much larger lateral displacements than the perimeter in-plane walls, as shown in Figure 5. Due to this behavior, the dynamic characteristics (e.g., fundamental period) and critical nonlinear behavior is associated with the movement of the diaphragm, rather than the in-plane vertical lateral force resisting elements, typical of most building systems. As such, the key structural performance characteristics for RWFD structures include the following:

- Nonlinear demands on the diaphragm (i.e., diaphragm ductility)
- Wall-to-diaphragm anchorage that transfers out-of-plane forces
- Out-of-plane displacement of the structural walls.

The interaction of the diaphragm and surrounding perimeter walls is highlighted in Figure 6.

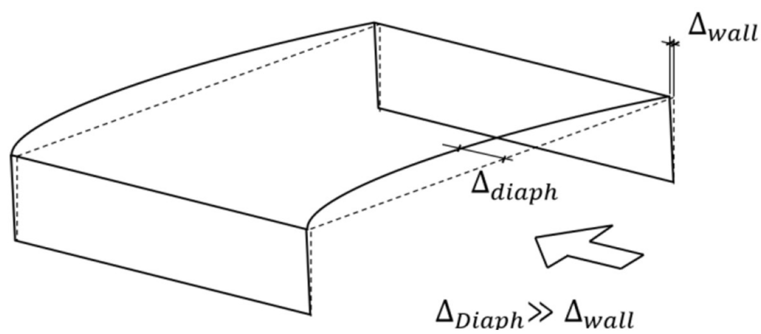

Figure 5. Basic comparison of in-plane wall and diaphragm lateral displacements due to seismic loading in rigid wall flexible diaphragm structures (Wade et al. 2018)

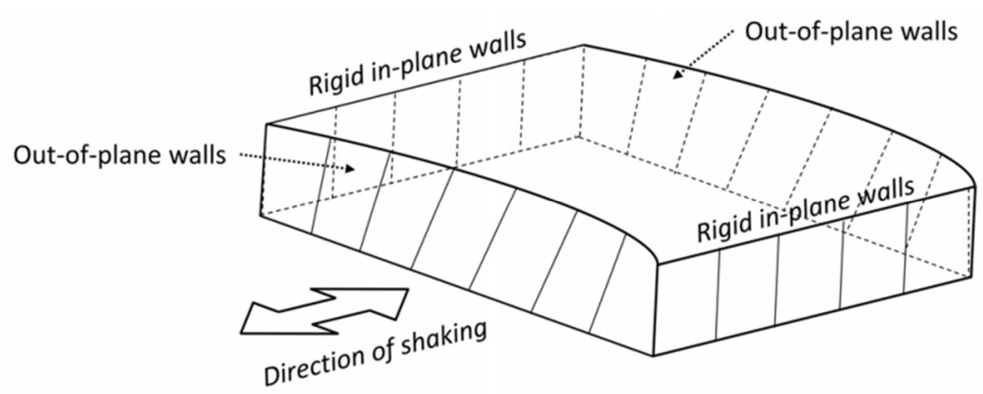

Figure 6. Interaction of diaphragm deflection with the perimeter walls (Lawson and Koliou, 2020)

1.2. Code Considerations for RWFD Structures

1.2.1. Adopted Design Approach for Diaphragm Design

The current analysis performs designs of RWFD archetypes according to the standard Equivalent Lateral Force (ELF) procedure outlined in ASCE 7-22 (ASCE, 2022) Sections 12.10.1 and 12.10.2 for diaphragms, chords and collectors. Importantly, seismic design loads for diaphragms are a function of R rather than R_{diaph}, where R depends to the LFRS according to 12.10.1 of ASCE 7-

22. The current study investigates the functional recovery response modification coefficient specific to the diaphragm, $R_{diaph,fr}$, to be more in line with the current understanding of RWFD structures. Historically, out-of-plane anchorage connections have resulted in RWFD collapses, following 1971 San Fernando and 1994 Northridge events, among others. This caused a large increase in wall anchorage design forces in the 1997 UBC, and remain largely unchanged in ASCE 7-22. As out-of-plane wall anchorage design forces have drastically increased, and have been shown to be generally adequate with recent analytical studies, the seismic performance of the diaphragm itself is critical to the seismic performance of RWFD structures (Koliou et al. 2017).

The concept of using separate R factors for diaphragm design was introduced in ASCE 7-16 (ASCE, 2016) in Section 12.10.3, which is a required procedure for pre-cast concrete diaphragm design. Most recently, ASCE 7-22 added Section 12.10.4, an optional procedure for one-story RWFD structures. The provisions of Section 12.10.4 incorporate the results of the FEMA P-1026 project (FEMA, 2015; 2021), which evaluated traditional diaphragm design (i.e., ASCE 7-22 Section 12.10.1) and developed an alternative approach based on the most recent experimental data and analytical capabilities. Targeting the appropriate response modification factor for diaphragm design ($R_{diaph,fr}$) is a key parameter of the current study.

The prequalification assessment for RWFD structures documented in this report is primarily performed following the procedure outlined in ASCE 7-22 (ASCE, 2022) Sections 12.10.1 and 12.10.2 for diaphragms, chords, and collectors, but with the response modification coefficient, R, replaced by the functional recovery response modification coefficient for design of diaphragms, $R_{diaph,fr}$. The proposed functional recovery seismic performance factors are also checked for compliance against the SCSD acceptance criteria using the alternative diaphragm design provisions of ASCE 7-22 Section 12.10.4. The application of the ASCE 7-22 Section 12.10.3 alternative diaphragm design provisions to the design of the archetypes and the resulting seismic provisions was not considered in this study.

1.2.2. Recent Evolution of the Flexible Steel Diaphragm Design

The treatment of flexible bare steel deck diaphragms within the structural engineering community has changed drastically in recent years. This is reflected in the time span between the first (2015) and second (2021) editions of the FEMA P-1026 report, which was originally developed only for wood structural panel diaphragms. It is also reflected in the tremendous amount of research on steel diaphragm connections, sub-assemblies and full specimen testing in that time span (O'Brien et al. 2017; Schafer et al. 2018; Schafer, 2019; Eatherton et al. 2021; Torabian and Shafer 2021). Based on extensive experimental results, the American Iron and Steel Institute has developed special seismic detailing requirements in the AISI S400-20 document (AISI, 2020, Section F3.5) that provide designers with a reliable procedure to ensure ductility capacity in bare steel deck diaphragms. The prescriptive detailing in AISI S400 combines the lessons learned from collected experimental evidence, especially in terms of primary and sidelap connection details. AISI S400-20 also includes qualification procedures for new connection types to meet special seismic detailing requirements. Finally, ASCE 342-22 (AISC, 2022) now includes nonlinear modeling and acceptance criteria for treating bare steel deck diaphragms as deformation-controlled based on synthesis of a similar experimental database (Wei et al. 2019). Prior to AISC 342-22/ASCE 41-23 (AISC, 2022; ASCE, 2023), bare steel deck diaphragms were treated as force-controlled elements in ASCE 41.

2. ANALYSIS METHODS

The methods used to perform the functional recovery analyses are presented in this section. Discussion of performing design iterations and acceptance criteria for the RM-RWFD system are discussed in Section 2.1. Background information on the fragility functions used to estimate SCSD is provided in Section 2.2. The details of the archetype design space used for analysis are provided in Section 2.3. The estimation of structural responses, or engineering demand parameters (EDPs), is discussed in Section 2.4.

2.1. Design Iteration and Acceptance Criteria for Seismic Performance Factors

For each individual archetype, design iterations are carried out using values of $R_{diaph,fr}$ and $I_{p,fr,oop}$ across the ranges of 1 through R (i.e., up to the response modification coefficient used in life-safety design) and 0.7 through 1.75 (i.e., up to the prescribed $I_{p,fr}$ value for FRC A/B in Appendix A of the recommended NEHRP provisions), respectively. The Response Modification Factor, R, is 5 for special reinforced masonry bearing wall systems in SDC D, E and F, in accordance with Table 12.2-1 of ASCE 7-22 (ASCE, 2022). These design iterations are performed using the SP3 design engine. $I_{p,fr,oop}$ was selected as a primary prequalification variable instead of the design drift limit, $\Delta_{a,diaph,fr}$, because in the prequalification assessment performed, story drift ratio is not a substantial cause of safety-critical structural damage. Instead, diaphragm damage is predicted from the diaphragm ductility demand, which is a more direct measure of diaphragm damage.

In each performance group, the combination of $R_{diaph,fr}$ and $I_{pfr,oop}$ is deemed to be acceptable if the mean P[SCSD] is less than 10%, and the maximum P[SCSD] across all archetypes in the performance group is less than 20% for quantifying the functional recovery seismic performance factors for Functional Recovery Category (FRC) A, B and C. For FRC D, the mean and maximum P[SCSD] across all archetypes in a performance group must be less than 15% and 25%, respectively. The recommended design values for a particular system are taken as the most restrictive across all performance groups, rounded to the nearest increment considered (0.5 for $R_{diaph,fr}$ and 0.25 for $I_{pfr,oop}$).

The requirements of the proposed Section A.8 procedures of the 2026 NEHRP Provisions impose that $R_{diaph,fr}$ and $\Delta_{a,diaph,fr}$ shall not be taken less than $R_{diaph}/1.5$ and 1.25% for FRC A, B and C and $R_{diaph}/1.25$ and 1.75% for FRC D, with R_{diaph} as specified in ASCE/SEI 7-22 Section 12.10.4.2.1. These "judgment-based" upper limits on seismic performance factors correspond to values required for Risk Category IV (FRC A, B, and C) and Risk Category III (FRC D) structures when performing life safety design.

2.1.1. *Safety-Critical Structural Damage (SCSD)*

The assigned safety class governs the triggering of SCSD for a given component and damage state according to the ATC-138 methodology (ATC, 2021). The safety class controls the percentage of components in each story and direction that can be in each damage state or greater before triggering SCSD. A summary of the ATC-138 safety class descriptions and acceptance thresholds is shown in Table 3.

Table 3. ATC-138 safety-class definitions for triggering SCSD (ATC, 2021).

Safety Class	Description	Acceptance Threshold[a]
0	Slight damage that is not a safety concern and will never trigger an unsafe placard	N/A
1	Moderate damage that may be visually concerning, but does not substantially reduce the lateral strength of the component.	50%
2	Severe damage that causes substantial loss of lateral strength of the component, but does not substantially reduce its vertical load carrying capacity.	25%
3	Severe damage that compromises both lateral and vertical load carrying capacity of the component.	10%

[a] Percentages reflect the upper quantity of components, in each story and direction, that can be in a safety class of interest before triggering safety-critical structural damage (SCSD). The safety critical structural damage check is performed independently for each independent system in the building (e.g., the gravity vs. lateral system).

2.1.2. *System Specific SCSD Considerations*

The four main groups of components that are considered for RM-RWFD building SCSD assessment are the roof diaphragm, the diaphragm-to-wall anchorage, out-of-plane response of perimeter walls and in-plane behavior of intermediate resistance lines (if applicable). The specific components and damage state safety class assignments are discussed in Section 2.2.

2.2. Fragility Functions for the RM-RWFD System

Fragility functions are used to relate structural responses to likely damage and consequences. Fragility functions are commonly modeled by a lognormal distribution defined by a lognormal mean (θ) and standard deviation (β). For a given structural component, sequential damage states (DSs) can be represented by individual fragility functions that characterize the likelihood of a distinct level of damage, the corresponding level of repair effort, and the associated consequences. Additionally, damage states may be mutually exclusive, where a single fragility function may be used to represent multiple outcomes (i.e., sub-damage states) where the likelihood of each is given a weighting that sums to unity (e.g., 0.25 + 0.75 = 1). The fragility functions used in the current study will employ both sequential and mutually exclusive damage-state definitions. More general background information on fragility functions and damage state development can be found in FEMA P-58-1 (FEMA, 2018a).

The development of fragility functions for RWFD structures was part of a collaborative effort between Haselton Baker Risk Group, John Lawson (Cal Poly San Luis Obispo), and Maria Koliou (Texas A&M University) to enable FEMA P-58 assessments of tilt-up buildings in seismic areas (Wade et al. 2018). The general approach to fragility development attempted to follow and incorporate the SEAONC *Guidelines for Seismic Evaluation and Rehabilitation of Tilt-up Buildings and Other Rigid Wall/Flexible Diaphragm Structures* wherever possible.

The following sub-sections provide details on the structural component fragility functions, including:

- Wood roof diaphragms;
- Out-of-plane wall-to-diaphragm anchorage;
- Out-of-plane walls.

Notably, in-plane walls are considered rugged for the analysis of RWFD systems because they are often very long and their designs are typically governed by minimum reinforcing and out-of-plane bending requirements, rather than in-plane shear demand. While the assumption that in-plane walls are rugged is consistent with typical RWFD construction and observations from past earthquakes, it is entirely possible to design a RWFD building with enough wall openings to make in plane deflection and/or shear demand the controlling factors in the design of the walls. Such cases are not assessed here; however, they are addressed by requiring R_{fr} specific to the lateral force resisting system (i.e. masonry shear walls).

2.2.1. Wood Roof Diaphragm Fragilities

Wood roof diaphragm fragilities were developed as part of Chapter 6 of FEMA P-58 Volume 2 (Implementation Guide) that illustrates different techniques for deriving fragility functions based on calculation, with a wood diaphragm tilt-up building used as an example structure (FEMA, 2018b). The sample structure assumed a fully blocked and chorded wood structural panel diaphragm, similar to detailing provided in modern wood diaphragms for RWFD structures in seismic areas (Lawson, 2007; 2008).

The definition of damage states considered available testing (Tissell, 1967) and expected damage attributed to different performance levels in ASCE 41-06 (ASCE, 2006). Illustrations of nail pull out and panel buckling observed from testing by Tissell (1967) are provided in Figure 7. ASCE 41-06 Table C1-4 damage descriptions for wood diaphragms are summarized in Table 4 for different performance levels. Three sequential damage states (DS) are defined for wood diaphragms for fragility development:

- DS1 - Tearing of roofing materials and flashing at supports. Some nail slippage and withdrawal at the diaphragm center and corners.
- DS2 – In addition to DS1 damage, nail pull out, framing splitting and plywood tearing extends into the diaphragm.
- DS3 - In addition to damage described for DS1 and DS2, plywood panels pull free of sub-framing and framing splits over approximately 25% of the diaphragm span at each diaphragm support.

The fragility functions are developed using the diaphragm ductility demand as an engineering demand parameter (EDP), which is calculated as the total diaphragm deflection (Δ) divided by the yield deflection (Δ_y). The capacity of wood diaphragms is approximated using the "idealized backbone" defined in ASCE 41-06 Table 8-4 for diaphragms consisting of blocked and chorded wood structural panel with an aspect ratio less than or equal to 3. Median values of diaphragm ductility for each damage state were estimated by comparing damage descriptions for ASCE 41-06 performance levels to the assumed damage states for fragility development. DS1 was attributed a median value based on the mid-point between IO and LS performance levels on the ASCE 41-06 backbone. Similarly, DS2 and DS3 medians were estimated as just beyond the LS and CP thresholds, respectively. An illustration of the assumed damage state medians for wood roof diaphragms in comparison with the ASCE 41-06 backbone is shown in Figure 8.

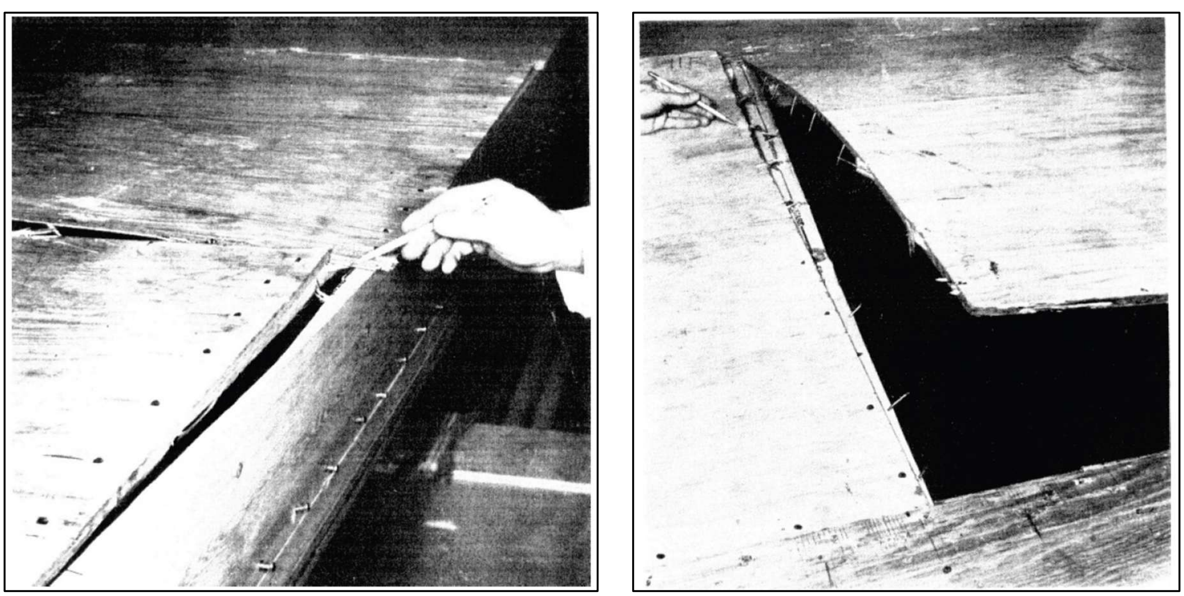

a) b)

Figure 7. Ex. of observed wood diaphragm damage from experimental testing: a) nail pull out; b) panel buckling (Tissell, 1967)

Table 4. Damage descriptions for wood diaphragms at various performance levels in ASCE 41-06 Table C1-4 (ASCE, 2006)

Immediate Occupancy (IO)	Life Safety (LS)	Collapse Prevention (CP)
No observable loosening or withdrawal of fasteners. No splitting of sheathing of framing.	Some splitting at connections. Loosening of sheathing. Observable withdrawal of fasteners. Splitting of framing and sheathing.	Large permanent distortion with partial withdrawal of nails and extensive splitting of elements.

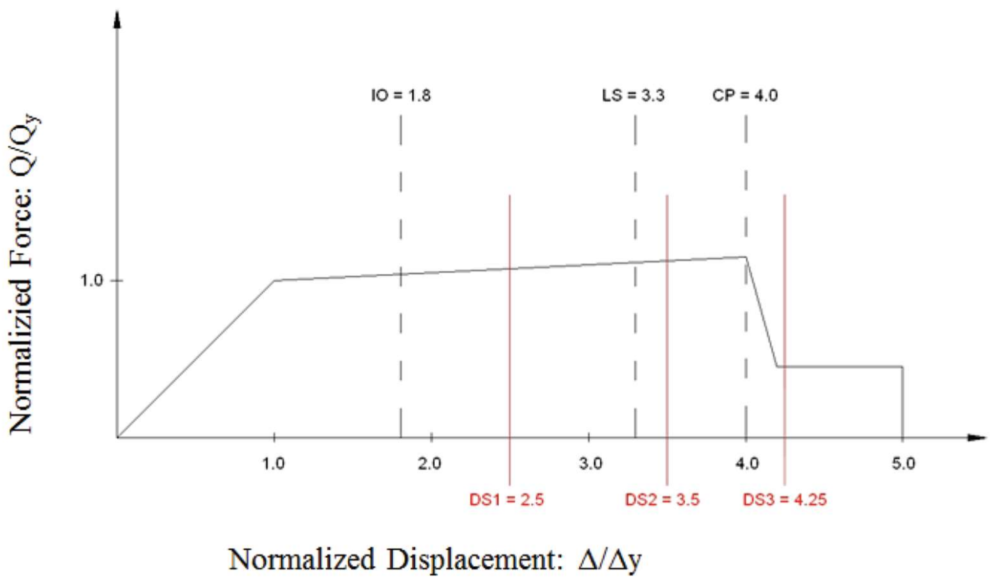

Figure 8. Comparison of assumed wood diaphragm damage state medians with different performance levels from ASCE 41-06 in FEMA P-58-2 (FEMA, 2018b)

The dispersion (β), or lognormal standard deviation, attributed to each of the damage states assumes a value of 0.5. This is derived using the procedure for ductility-limited damage states in FEMA P-58 Volume 1 Section 3.8.4 (FEMA, 2018a). A brief derivation of the calculations and assumptions used to obtain β is provided in Figure 9. Notably, a total dispersion value of 0.5 is also the default value for defining fragilities using code-based limit states in FEMA P-58-1 3.8.4.

Estimate dispersion associated with first yield, β_1 (FEMA P-58-1 Eqn. 3-3):

$$\beta_1 = \sqrt{\beta_D^2 + \beta_M^2 + \beta_C^2} = \sqrt{0.1^2 + 0.2^2 + 0.1^2} = 0.24$$

- β_D – variability in design equations (P-58-1 default for complex ductile behavior)
- β_M – material variability (P-58-1 Table 3-4 default for visually graded wood)
- β_C – construction quality uncertainty (P-58-1 Table 3-5, average quality control, moderate sensitivity)

Estimate dispersion in each damage state, β (FEMA P-58-1 Eqn. 3-4):

$$\beta = \sqrt{\beta_1^2 + 0.16} \leq 0.6 = \sqrt{0.24^2 + 0.16} = 0.47 \approx 0.5$$

Figure 9. Derivation of the total dispersion values attributed to damage states for wood roof diaphragms (FEMA, 2018b)

A summary of the wood roof diaphragm fragility functions and corresponding safety classes is provided in Table 5. DS1 is assigned to Safety Class 0. DS2 and DS3 are assigned to Safety Class 1 and 2, respectively. Plots of fragility functions for wood structural panel roof diaphragms are provided in Figure 10. Additional details on the development of these fragilities can be found in Section 6.3.1 of FEMA P-58-2 (FEMA, 2018b).

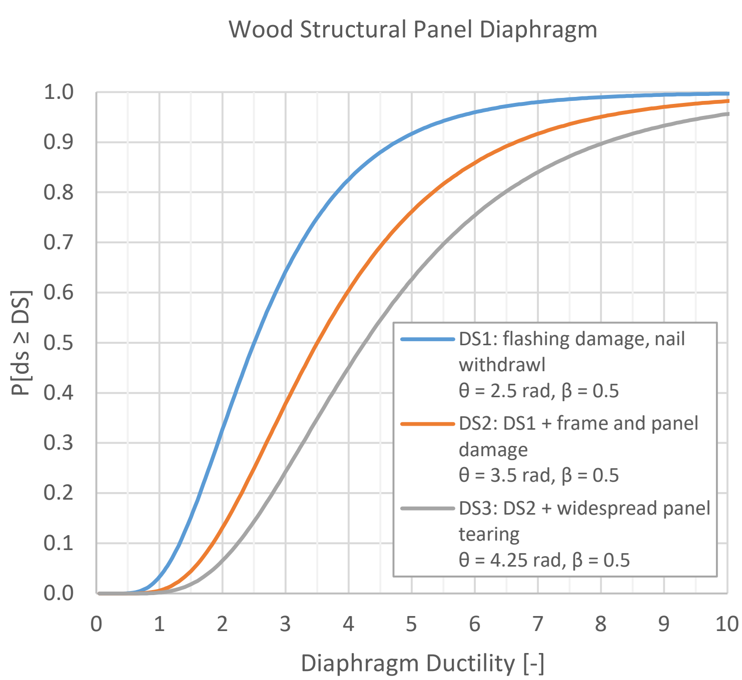

Figure 10. Fragility functions for wood structural panel roof diaphragms. Damage state details are provided in Table 5.

Table 5. Wood structural panel roof diaphragm fragility damage states and corresponding safety classes.

Damage State	Median (θ)[a]	β	Safety Class[b]	Damage Description	Repair Measures
DS1	2.5	0.50	0	Tearing of roofing materials and flashing at supports. Some nail slippage and withdrawal at the diaphragm center and corners.	Remove the existing flashing and 4-feet of roofing material along the wall. Remove damaged nails and install new nails where no splitting of the frame has occurred (25% of nails over the 4-foot width). Remove and replace plywood and framing including ledgers at split framing or damaged plywood (25% of the 4-foot width).
DS2	3.5	0.50	1	In addition to DS1, Nails pull out, framing splitting and plywood tearing extends into the diaphragm.	Extend DS1 repairs to an 8-foot width, remove damaged nails and install new nails where no splitting of framing occurs (25% of nails over 8-foot width of diaphragm along wall). Remove and replace plywood and framing including ledgers at split framing or damaged plywood (25% of 8-foot width of diaphragm along wall).
DS3	4.25	0.50	2	In addition to damage described for DS1 and DS2, plywood panels pull free of sub-framing and framing splits over approximately 25% of the diaphragm span at each diaphragm support.	Remove and replace roofing, flashing, plywood, framing (girder not replaced) over 25% of diaphragm span and full depth of wall at each diaphragm support.

[a] Fragility function is a lognormal distribution with median and standard deviation of θ and β, respectively. The EDP is diaphragm ductility (Δ/Δ_y), where Δ_y is determined according to ANSI/AF&PA SDPWS-2005 Equation 4.2.1 as illustrated in Section 6.3.1 of FEMA P58-2.
[b] SC 1 = 50%, SC 2 = 25%, SC 3 = 10% allowable quantity of damaged components per direction per story; SC 0 cannot cause SCSD.

The current fragilities for wood roof diaphragms are based on engineering judgment of generalized backbones in ASCE 41-06, which are unchanged in ASCE 41-23 (i.e., d = 4, e = 5, c = 0.3). The experimental basis for the ASCE 41 *backbones* for wood diaphragms is not clearly stated in ASCE 41, yet the American Plywood Association's *Research Report 138 – Plywood Diaphragms* (Tissell and Elliot, 2001) is commonly referenced in all versions of ASCE 41 commentary (i.e., ASCE 41-06, 41-13, 41-17, 41-23). The APA 138 report has been revised numerous times as more testing has become available, and the latest version still includes early testing conducted in the 1950's (Countryman, 1952; 1955). Prestandard commentary of FEMA 274 (FEMA, 1997) also cites the APA Report 138, yet also cites the early testing conducted by the Agbabian-Barnes-Kariotis Joint Venture (ABK, 1981). It is likely that the ABK testing was the initial source for developing backbone parameters for older wood diaphragms construction (e.g., those without wood structural panel), yet this early test campaign did include panelized wood sheathing specimens (Carter et al. 1993; Whitney and Agrawal, 2015).

2.2.2. Out-of-Plane Wall-to-Diaphragm Anchorage Fragilities

Fragility functions for out-of-plane wall-to-diaphragm anchorage (OOP anchorage) are developed as calculated code-based limit state fragilities, as defined in FEMA P-58-1 Section 3.8.4. Code-based fragilities are used to relate a design requirement (e.g., bending resistance, anchorage force, etc.) to the actual capacity expected for a designed component or assembly. The basic process for estimating a median capacity (θ) using the code-based limit state procedure is summarized in Figure 12. Importantly, the code-based limit state procedure requires fixed values of dispersion ($\beta = 0.5$) and sensitivity to construction quality ($C_q = 0.5$), which only leaves the required design resistance (ϕR_n in Figure 12) and nature of the failure mode (e.g., ductile or brittle) to be determined. FEMA P-58-1 Equations (3-1) and (3-2) (see Figure 12) provide estimates for median (expected) capacity for ductile and brittle failure modes with respect to required design resistance. Ductile failure modes expect less of a margin between design resistance and expected capacity compared to brittle failure modes. This is analogous to the difference in resistance factors (ϕ) for designing a simple RC beam for flexure ($\phi = 0.9$) versus designing for shear ($\phi = 0.75$). With all other parameters fixed (i.e., $\beta = 0.5$ and $C_q = 0.5$), the increase in the median capacity from design resistance is a factor of 1.4 and 2.0 for ductile and brittle connections, respectively, according to the procedure.

In the case of OOP anchorage, ASCE 7-22 Equation 12.11-1 determines the required design resistance, F_p (ϕR_n in Figure 12), for life safety design, and is repeated below in Eq. (1):

$$F_p = 0.4 S_{DS} k_a I_e W_p \geq max\left(0.2 k_a I_e W_p,\ 5\, lb/ft^2\right) \tag{1}$$

For functional recovery design, the building importance factor (I_e) must be replaced by I_{pfr} according to the exception in Section A.8.2 of the 2026 NEHRP Provisions, and S_{DS} must be replaced by the short period spectral acceleration for the FRE_R (S_{DSfr}). Normalizing by tributary weight, the controlling equation for functional recovery design is shown in Eq. (2):

$$F_p / W_p = 0.4 S_{dsfr} k_a I_{pfr} \tag{2}$$

where the lower limits shown in Eq. (1) do not control at the FRE_R ($S_{DSfr} = 1.25$). Notably, the amplification factor, k_a, is always taken as the upper limit of 2.0 for RWFD structures using SP3, which represents a building length of 100 ft or more.

Given that there is no force reduction parameter in ASCE 7-22 Equation 12.11-1, OOP anchors have no specified ductility requirements. Furthermore, out-of-plane design for walls are treated as force-controlled actions in ASCE 41. Therefore, to convert the required design strength to the expected strength for the out-of-plane wall anchorage, a brittle failure mode is assumed and a 2.0 overstrength factor is used in the median capacity from design resistance and the median expected anchorage strength (θ_{OOP}) is given by Eq. (3):

$$\theta_{OOP} = 2\left[{}^{F_p}\!/_{W_p}\right] \tag{3}$$

where the normalized design capacity (F_p/W_p) is defined in Eq. (2). See a typical OOP wall connection illustrated in Figure 11.

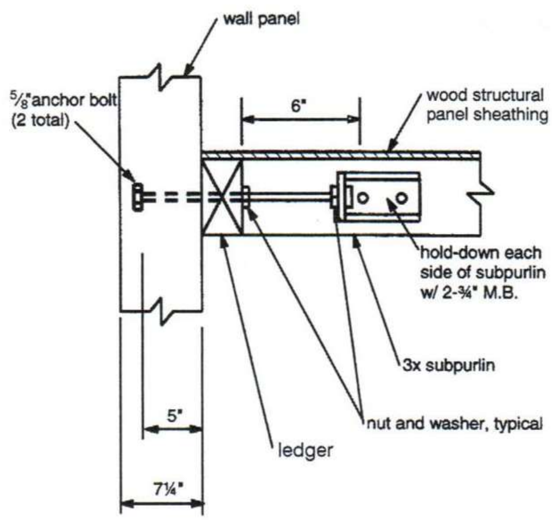

Figure 11 - Typical out-of-plane wall-to-diaphragm connections for flexible wood roof diaphragms.

Fragility functions for out of plane wall anchorage consist of two sequential damage states. DS1 has a median equal to the expected anchorage strength (θ_{OOP}) while DS2 has a median associated with 1.2 times the expected anchorage strength ($1.2\theta_{OOP}$) (Lawson, 2017). Both damage states are associated with failure of the anchorage connections and assigned to Safety Class 3, with DS2 representing more widespread failures compared to DS1. A summary of the out-of-plane anchorage fragility functions, and corresponding safety classes, is provided in Table 6.

Code-Based Limit States

In some cases, there may be insufficient information to calculate the capacity of a component. For example, information on the anchorage capacity of a piece of equipment may not be available because the anchorage has not yet been designed, or in the case of an existing installation, the details of the anchorage are not known. In such cases, the code-based design strength for the code in effect at the time of installation can be used to establish the capacity of the component. The following procedure can be used:

1. Identify the governing code for the installation, and compute the design strength (or displacement capacity) in terms of a convenient demand parameter, such as spectral acceleration, force, or story drift ratio. The code-based capacity is then taken as the presumed value of ϕR_n.
2. Decide whether the damage state is a ductile or brittle failure mode. If it is unknown which is likely, a separate calculation can be performed for ductile and brittle assumptions, and the results averaged.
3. Assign a default dispersion of $\beta = 0.5$.
4. If the mode is considered ductile, determine the median value of θ using use Equation 3-1. If the mode is considered nonductile, determine the median value of θ using Equation 3-2. In either case, a value of $C_q = 0.5$ should be assumed.

$$\theta_{ductile} = C_q e^{(2.054\beta)} \phi R_n \qquad (3\text{-}1)$$

$$\theta_{brittle} = C_q e^{(2.81\beta)} \phi R_n \qquad (3\text{-}2)$$

Figure 12. Definition and summary of the Code-Based Limit State procedure of FEMA P-58-1 (FEMA, 2018a) used for estimating capacity of wall-to-diaphragm anchorage.

Table 6. Out-of-plane wall anchorage fragility damage states and corresponding safety classes.

Damage State	Median (θ)[a]	β	Safety Class[b]	Damage Description	Repair Measures
DS1	θ_{OOP}[c]	0.5	3	Connections fail at one to several bays near the in-plane walls causing the bay nearest the out-of-plane wall to collapse into the building.	Demo the fallen diaphragm as well was the surrounding diaphragm damage. Replace the damaged diaphragm, out-of-plane wall connections.
DS2	$1.2\theta_{OOP}$	0.5	3	Connections fail along an entire wall line precipitating collapse of the wall outward and the diaphragm to the floor of the building.	Demo the fallen wall and diaphragm as well as surrounding damaged components.

[a] Fragility function is a lognormal distribution with median and standard deviation of θ and β, respectively. The EDP is out-of-plane anchorage force.
[b] SC 1 = 50%, SC 2 = 25%, SC 3 = 10% allowable quantity of damaged components per direction per story; SC 0 does not result in SCSD.
[c] θ_{OOP} is taken as twice the ASCE 7-22 Eqn. 12.11-1 normalized design force (i.e., F_p/W_p) adjusted for the FRE_R

2.2.3. Out-of-Plane Wall Fragilities

Fragility functions for out-of-plane perimeter walls were developed based on testing of slender concrete and masonry walls conducted by the ACI-SEAOSC Task Force on Slender Walls (ACI-SEAOSC, 1982). Test data interpretation and the definition of damage states was conducted in collaboration with John Lawson during the development of the RWFD module within the SP3 program (Lawson, 2017; Wade et al. 2018).

The tests consisted of 12 reinforced concrete specimens and 18 reinforced masonry specimens. Specimens were tested in full scale using monotonic out-of-plane loading with constant axial load. Out-of-plane slenderness ratios (h/t) ranged from 30 to 60 (FEMA, 1999). Monotonic loading was achieved by using an air bag apparatus to simulate wind and seismic loading (see Figure 13a). Examples of specimens during testing are shown in Figure 13b. Notably, these tests were used to reevaluate calculations and requirements for out of plane walls in ACI 318-08 (ACI, 2008; Lawson and Lai, 2010).

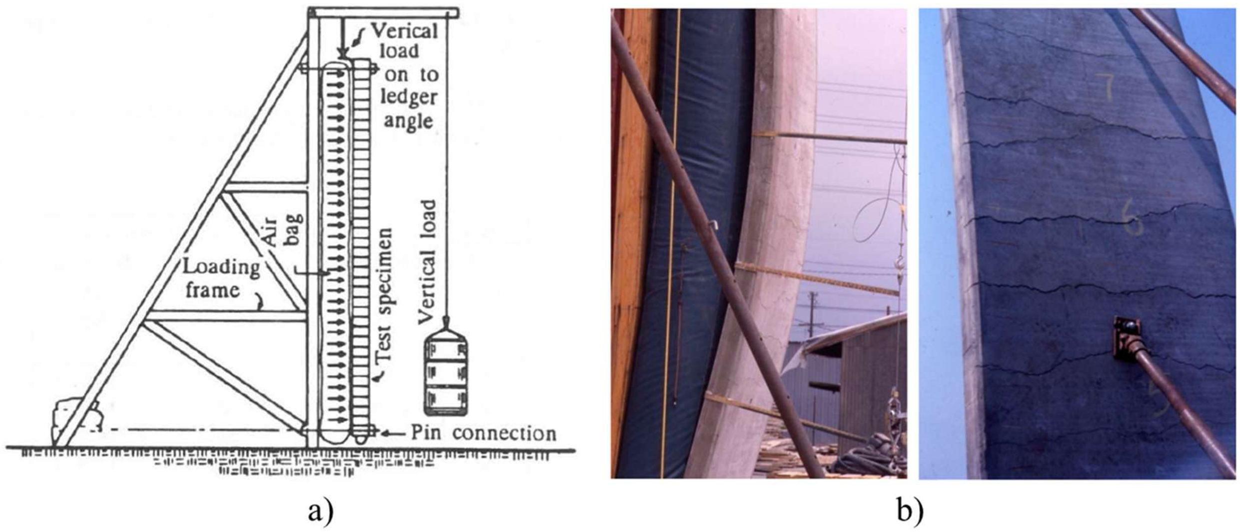

Figure 13. Experimental basis for out-of-plane wall fragilities: a) Static air bag apparatus (Adham et al. 1988); b) Example wall specimens during out of plane testing (Lawson and Lai, 2010).

Fragility functions for out of plane (OOP) wall assemblies consist of two sequential damage states using the OOP story drift ratio (SDR_{OOP}) as an EDP. OOP story drift ratio is defined as the mid-height deflection divided by the wall height at the diaphragm connection, as shown in Figure 14. DS1 represents significant cracking that requires epoxy injection repair. DS2 represents similar damage to DS2 but includes residual deformation that requires realignment or replacement of the wall panel. A summary of the out-of-plane wall fragility functions, and corresponding safety classes, is provided in Table 7. Plots of fragility functions for out-of-plane wall assemblies are provided in Figure 15.

Table 7. Out-of-plane wall assembly fragility damage states and corresponding safety classes.

Damage State	Median (θ)[a]	β	Safety Class[b]	Damage Description	Repair Measures
DS1	2.00%	0.5	0	Residual cracking requiring epoxy injection	Epoxy inject residual cracks.
DS2	3.00%	0.5	1	DS1 + residual drift requiring realignment	Straighten and repair the wall or replace the panel.

[a] Fragility function is a lognormal distribution with median and standard deviation of θ and β, respectively. The EDP is out-of-plane story drift ratio (SDR_{OOP} in Figure 14).
[b] SC 1 = 50%, SC 2 = 25%, SC 3 = 10% allowable quantity of damaged components per direction per story; SC 0 does not result in SCSD.

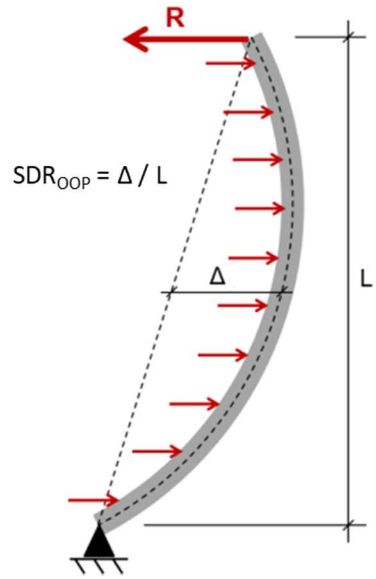

Figure 14. Definition of out of plane drift ratio (SDR_{OOP}) for wall assemblies (Image adapted from Wade et al. 2018).

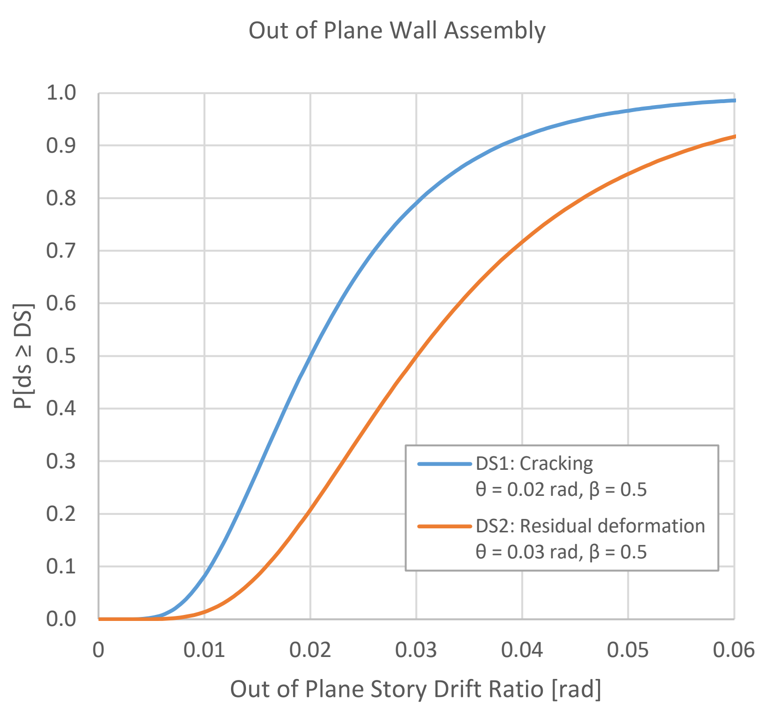

Figure 15. Fragility functions for out of plane wall assemblies. Damage state details are provided in Table 7.

2.3. Archetypes Considered for Analysis

To determine the $R_{diaph,fr}$ and $I_{pfr,oop}$ that results in acceptable functional recovery performance, an archetype space is broken up into performance groups, analyzed, and the overall parameters are determined by the worst-case of the performance groups. This is similar to the FEMA P-695 methodology used for quantifying performance factors for life-safety (FEMA, 2009) and is in accordance with the proposed Section A.8 procedures of the 2026 NEHRP Provisions.

2.3.1. Building Configuration and Structural Component Population

The structural configurations included in the archetype design space are an extension of those considered within the FEMA P-1026 (FEMA, 2021) document to investigate the adequacy of traditional design procedures for RWFD buildings and provide supporting information on the alternative design procedure of ASCE 7-22 Section 12.10.4 (ASCE, 2022). The FEMA P-1026 study analyzed numerous archetypes using the FEMA P-695 (FEMA, 2009) methodology to assess the collapse performance of RWFD structures. The detail variations include the following:

- Wall height
- Plan size
- Plan aspect ratio
- Presence of interior lateral force resisting lines
- Type of interior lateral force resisting system (as applicable).

Archetypes consider 24-foot and 30-foot wall heights from the top of grade to the roof diaphragm level. All archetypes assume that the total wall height is extended three feet above the roof diaphragm level (i.e., a 3-foot-tall parapet is assumed). Wall height affects both the design loading and the estimated fundamental period of the system during assessment.

The plan sizes are categorized into small, large, and very large. Small plan sizes consider aspect ratios of 1 and 2 with plan dimensions of 100 ft by 100 ft and 200 ft by 100 ft, respectively. Large plan sizes consider aspect ratios of 1 and 2 with plan dimensions of 400 ft by 400 ft and 400 ft by 200 ft, respectively. The very large plan size is assumed to be at a constant aspect ratio of 2 with dimensions of 800 ft by 400 ft. Diaphragm aspect ratios are limited to a value of 2.0 for the current study. Although larger aspect ratios are common in areas of low to moderate seismicity (e.g., 3:1 and 4:1), diaphragm designs with larger aspect ratios can become unfeasible in areas of high seismicity due to connection detail limitations (Koliou et al. 2016a). Further, FEMA P-1026 analysis observed that the diaphragm span had a much larger effect on the periods of the RWFD compared to the aspect ratio due to diaphragm behavior being governed by shear deformation (FEMA, 2021). Based on these two points, the varied plan dimensions and assumed aspect ratios of 1 and 2 are deemed adequate to investigate the required seismic performance factors.

Archetypes with very large plan sizes (i.e., 800 ft by 400 ft) are assumed to contain interior lines of lateral force resistance. The interior lateral force resisting systems consider both reinforced concrete walls and ordinary steel concentrically braced frame (OSCBF) lines. An illustration of the different plan layouts for all archetypes is shown in Figure 16.

Each geometrical configuration (see Figure 16) considers a wood structural panel diaphragm. Discussion of bare steel deck diaphragms is provided in Section 4.

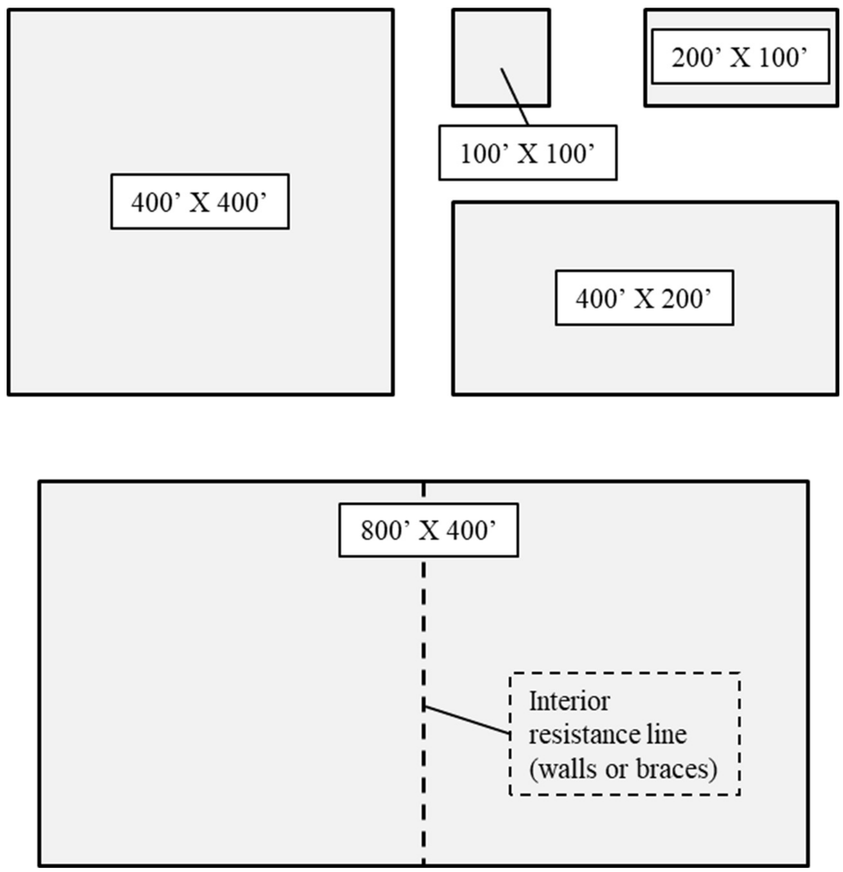

Figure 16. Plan configurations considered for special reinforced masonry rigid wall flexible diaphragm archetypes

An illustration of structural component population is shown for a 400 ft by 200 ft plan for loading perpendicular to the long dimension in Figure 17. Diaphragm units are populated as 50 ft^2 units. Out of plane wall sections are populated based on 25 ft long assemblies. Out of plane wall anchorage assemblies are populated based on a 50 ft spacing. This population scheme is typical for all archetypes and varies only based on plan dimensions of the roof diaphragm.

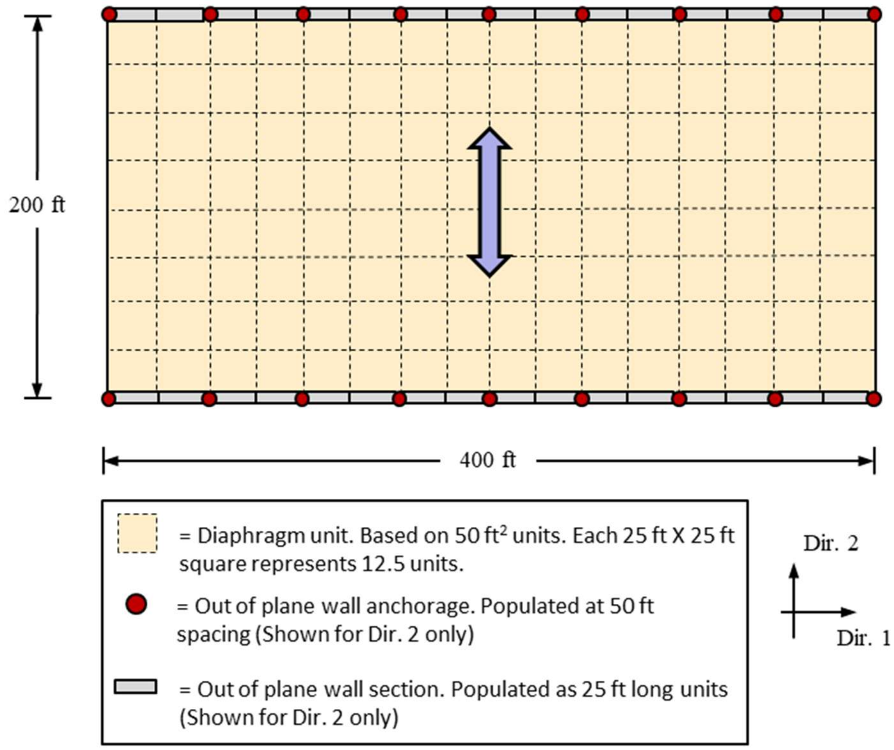

Figure 17. Structural component population for a 400 ft by 200 ft RWFD archetype. Population is only shown for loading in direction 2.

2.3.2. Performance Groups for RM-RWFD Systems

The different structural configurations are grouped into performance groups with similar expected seismic performance. This is similar to conducting FEMA P-695 analysis on a given lateral force resisting system for collapse safety. A total of four performance groups comprised of 12 individual archetype buildings are considered. The groups are then distinguished further according to building plan size and, for the very large plans, the use of either walls or braces for interior resistance lines. A summary of the RM-RWFD performance groups is shown in Table 8.

Table 8. Performance groups for special reinforced masonry rigid wall flexible diaphragm systems.

Performance Group	Archetype ID	Diaphragm Material	Plan Size	Plan Dimensions [ft]	Wall Heights [ft]	Interior Resistance Line?	Interior LFRS
PG1	1-W-A	Wood	Small	100 X 100	24	No	N/A
	1-W-B				30		
	1-W-C			200 X 100	24		
	1-W-D				30		
PG2	2-W-A	Wood	Large	400 X 200	24	No	N/A
	2-W-B				30		
	2-W-C			400 X 400	24		
	2-W-D				30		
PG3	3-W-A	Wood	Very Large - Interior Walls	800 X 400	24	Yes	Wall
	3-W-B				30		
PG4	4-W-A	Wood	Very Large - Interior Braces	800 X 400	24	Yes	Brace
	4-W-B				30		

2.4. Estimation of Structural Responses

The structural responses for the archetypes were determined using the SP3 Structural Response Prediction Engine (SRPE). The RWFD SRPE is documented in Wade et al. 2018. A summary of the analytical basis behind the SRPE as well as the quantification of different Engineering Demand Parameters (EDPs) is provided here.

The SP3 SRPE generates a simplified linear multi-degree-of-freedom model with strength and stiffness characteristics that are based on the building's layout and design requirements. Nonlinear responses are determined by first using the model to predict linear responses, and then modifying the linear responses to account for nonlinear behavior (damage) in the building. Modifications to account for nonlinear response depend on the strength of the building and are calibrated to Incremental Dynamic Analysis (IDA: Vamvatsikos and Cornell, 2002) results from high-fidelity nonlinear models with similar linear characteristics.

2.4.1. Analytical Basis Behind the RWFD Structural Response Prediction Engine (SRPE)

The RWFD SRPE is based on calibration to 16 different buildings modeled in OpenSees (McKenna et al. 2010). The models were developed by HBRG using calibration data provided by the same analysts and designers that conducted FEMA P-695 (FEMA, 2009) to assess the collapse potential of traditional RWFD design (ASCE 7-22 Section 12.10.1) and provide the basis for an alternative design procedure for RWFD structures (now ASCE 7-22 Section 12.10.4) as part of the

FEMA P-1026 project (FEMA, 2021). The RWFD SRPE was developed with building models representative of three different design eras: 1973 UBC and earlier, 1973 UBC to 1994 UBC, and 1997 UBC to present—noting that only the modern era archetypes will be discussed here. A summary of the different modern archetype buildings considered for SRPE calibration is provided in Figure 18. The modern RWFD building archetypes assumed a 30-foot wall height to the diaphragm connection with a 3-foot parapet. The models considered small and large plan sizes with aspect ratios of 1 and 2. Diaphragms are designed with wood structural panels and common nails.

All models were constructed using the same three-stage approach used in FEMA P-1026 archetypes, as shown in Figure 19. The first stage (Figure 19a) is to select diaphragm connection models from a database calibrated to experimental results of both wood and steel diaphragm connections (Koliou, 2014; Koliou and Filiatrault, 2017). The second stage (Figure 19b) explicitly models individual connections (with elements from stage 1) and roof (panel) materials in diaphragm sections or strips that correspond to differences in design detailing (e.g. fastener spacing; see Figure 18) that comprise the entire diaphragm. Cyclic loading is conducted on the full diaphragm assembly, allowing for representative macro elements to be calibrated to represent distinct sections of the diaphragm. The third stage assembles a simplified 2D model that utilizes the diaphragm macro elements from Stage 2 and includes the sources of mass and stiffness from both the roof diaphragm and the perimeter walls of the structure and numerically captures second order effects (i.e., P-delta effects). The simplified model greatly reduces the complexity associated with full diaphragm systems, suitable for running large sets of nonlinear response history analyses (NRHA). FEMA P-1026 and Koliou et al. (2015) provide further details on the background and execution of the three-stage modeling procedure.

All models were analyzed using the FEMA P-695 far-field ground motion set (FEMA, 2009) consisting of 44 ground motions (i.e., 22 horizontal pairs). Incremental Dynamic Analysis (IDA, Vamvatsikos and Cornell, 2002) was used to obtain a range of linear and nonlinear structural responses for calibration.

The key EDPs for structural response prediction of the RWFD systems are diaphragm ductility demand, out of plane wall anchorage demand, out of plane wall deflection, and peak roof acceleration. An illustration of the key EDPs used for RWFD structures is shown in Figure 20. The RWFD SRPE distinguishes between wood structural panel and bare steel deck diaphragm systems, reflecting the differences in modal properties (i.e., periods) and nonlinear behavior (e.g., yield drift, ductility capacity). An overview of the estimation of these EDPs is discussed in the following sub-sections.

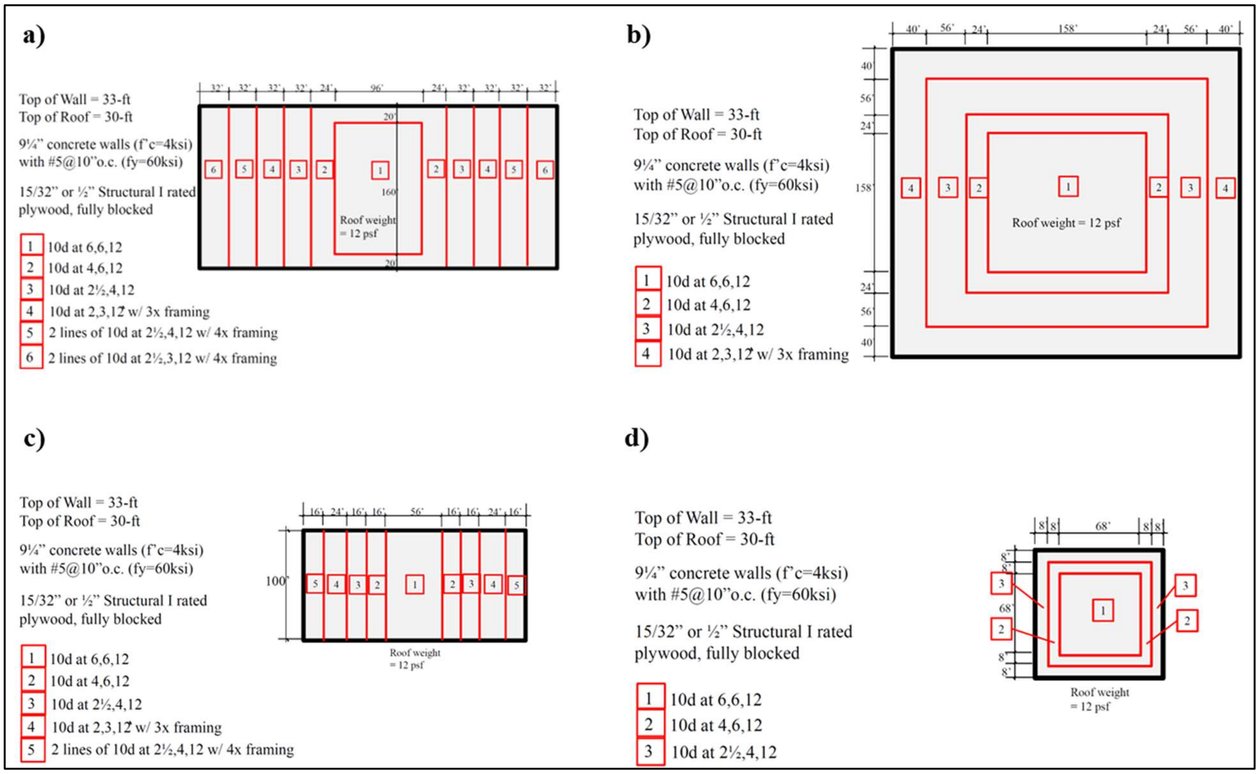

Figure 18. Design details of modern RWFD buildings used for calibration of the RFWD SRPE (Wade et al. 2018): a) 400 ft by 200 ft plan; b) 400 ft by 400 ft plan; c) 200 ft by 100 ft plan; d) 100 ft by 100 ft plan. Nailing regions assume 2x framing unless specified otherwise.

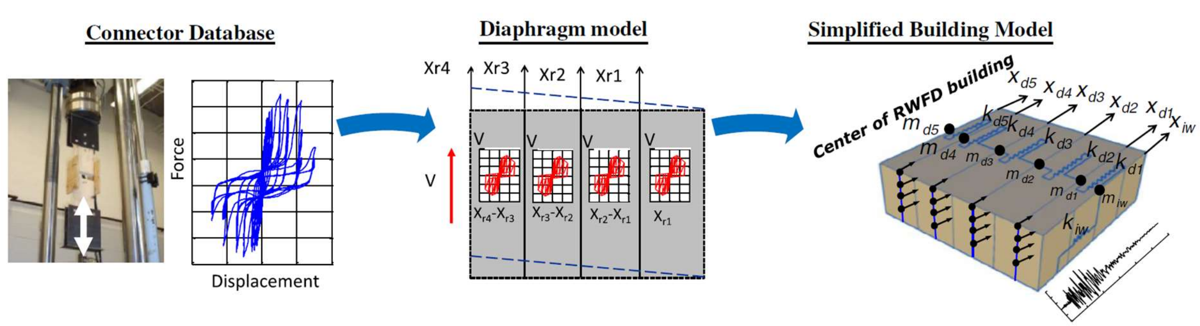

Figure 19. Summary of the three-stage analysis procedure used for nonlinear modeling of RWFD structures (Koliou et al. 2016a)

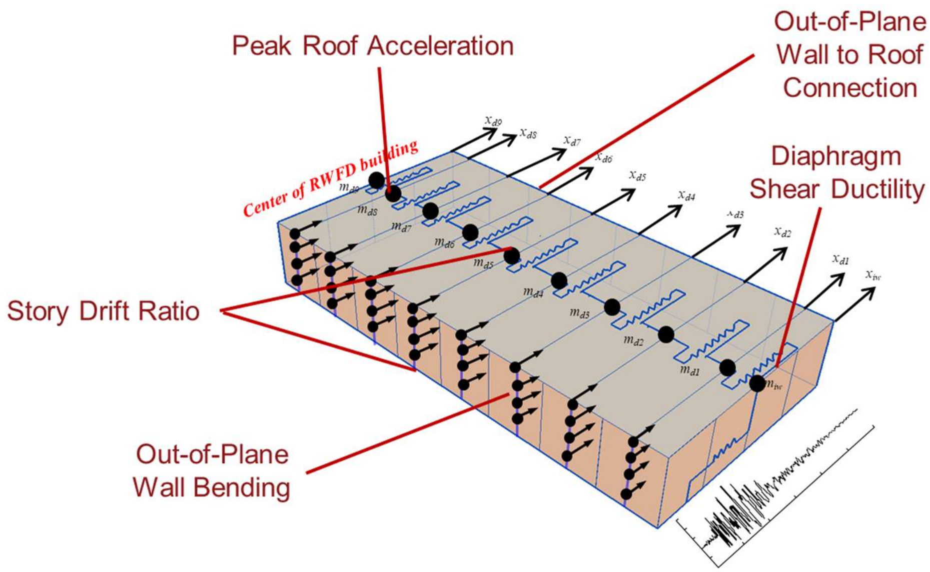

Figure 20. Illustration of key engineering demand parameters (EDPs) estimated by the RWFD SRPE. Image adapted from Koliou et al. (2016a)

2.4.2. Structural Properties Estimation

The primary response of RWFD buildings is the in-plane response of the diaphragm. Therefore, the in-plane fundamental period and strength of the diaphragm are the primary structural properties used for estimating global structural responses. The strengths of walls for bending in the out-of-plane direction is also determined for the purpose of estimating out-of-plane wall deflection demands.

The fundamental period is determined empirically, based on the equations proposed by Koliou et al. (2016a), as shown for wood and steel diaphragm buildings in Eq. (4) and Eq. (5), respectively:

$$T_{1,wood} = \frac{0.0019}{\sqrt{C_w}} h + 0.002L \tag{4}$$

$$T_{1,steel} = \frac{0.0019}{\sqrt{C_w}} h + 0.001L \tag{5}$$

where the first term represents the period contribution from in-plane walls and the second term includes the contribution of the diaphragm. The factor C_w is as defined in ASCE 7-22 Eq. 12.8-11, h is the height (in feet) of the walls, and L represents the diaphragm length (in feet) perpendicular to the direction of interest. Only the fundamental period in each direction is used for analysis in SP3 for RWFD structures.

Next, the expected strength of the diaphragm, accounting for overstrength, is estimated. This is done by first estimating the required design strength of the critical sections of the diaphragm. The required design strength is determined according ASCE 7-22 Section 12.10.1 and accounts for spectral values, response modification factor (R), and related values (e.g., Ie). The alternative diaphragm design provisions found in ASCE 7-22 Section 12.10.4 are also implemented in SP3, but they are not used for this study.

For a diaphragm with an aspect ratio greater than 1, the critical sections are at the extreme wall lines perpendicular to the long dimension of the diaphragm. An example of a critical section is highlighted in Figure 21. Required nail spacing and framing details (AWC, 2021) are selected in order to achieve the required shear strength. Very large diaphragms will require that interior resistance lines are provided to reduce the seismic shear on individual diaphragm sections. Overstrength applied to the diaphragm strength depends on nail spacing and diaphragm configuration. Tighter nail spacing has less inherent overstrength than wider spacing (AWC, 2021) and this is reflected based on the required diaphragm detailing of critical sections. Further, diaphragms with aspect ratios greater than 1 commonly have nailing controlled by the loading perpendicular to the long dimension, and this nailing is reduced toward the mid-span of the diaphragm (see Figure 21). The expected strength and overstrength of the opposite direction (loading parallel to the long dimension) considers that numerous nail spacings can comprise the critical section in this direction.

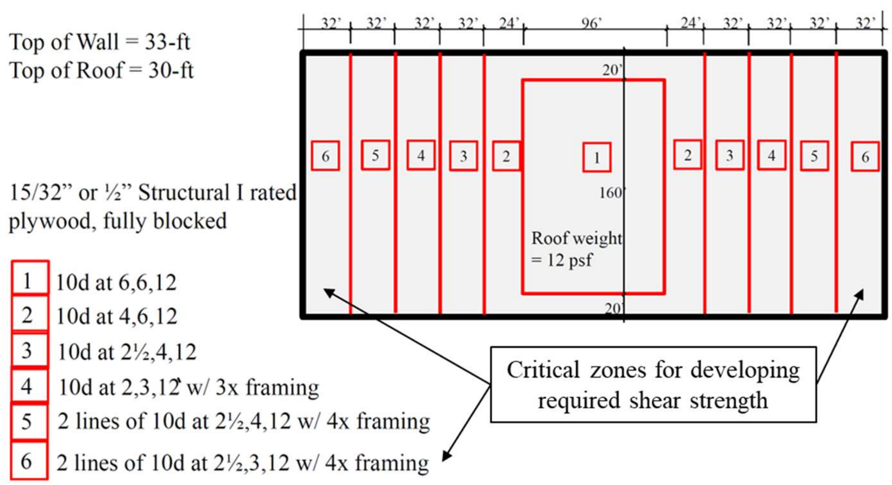

Figure 21. Example wood diaphragm design details for 400 feet by 200 feet plan and 30-foot wall height designed for R = 4, S_{DS} = 1.0g and S_{D1} = 0.6g (Figure adapted from FEMA, 2021)

Wall out-of-plane design strength is determined according to Section A.8 of the 2026 NEHRP Provisions. Neither ASCE 7-22 Section 12.11 nor the 2026 NEHRP provisions for design forces for out-of-plane walls include the seismic response coefficient, R. However, the 2026 NEHRP Provisions require out-of-plane wall forces to be scaled by the factor I_{pfr} in place of I_e, where I_{pfr} is determined based on the Functional Recovery Category (FRC) of the structure.

2.4.3. *Summary of EDP's predicted by the RWFD SRPE*

Several EDP's are predicted by the RWFD SRPE. The methods for determining each of these EDP's are calibrated based on the database of IDA results from the nonlinear OpenSEES models. The following is a summary of the EDP's that are used for analysis of RWFD's, listed in approximate order of importance.

Diaphragm Ductility Demand: Diaphragm ductility demand, which is defined as diaphragm peak displacement divided by diaphragm yield displacement, is predicted based on the ultimate strength of the diaphragm (V_{ult}) and the spectral acceleration at the fundamental period of the building $Sa(T_1)$, using a two-step process. First, a simple demand factor (S) is determined, $S = Sa(T_1)/V_{ult}$. When S ≤ 0.75, the diaphragm ductility demand is equal to 1.33S; this assumes that yielding occurs at S=0.75. For S > 0.75, the diaphragm ductility demand increases at a rate of 0.8S, due to hysteretic energy dissipation reducing the overall response; this reduction is calibrated based on the database of IDA results from the nonlinear OpenSEES models.

Peak Roof Acceleration and Out-of-plane Wall Anchorage Force Demand: Peak roof acceleration is determined from $Sa(T_1)$ and diaphragm ductility demand. Normalized wall anchorage force demands, measured in units of gravity (g), are determined directly from peak roof acceleration; they are ~25% less than peak roof acceleration, because wall flexibility in the out-of-plane direction reduces the demand on the connection. When minimal or no yielding is expected in the diaphragm (i.e. S < 0.75), only $Sa(T_1)$ is used to determine peak roof acceleration, which is somewhat higher than $Sa(T_1)$ due to higher mode effects. When diaphragm damage is expected (i.e. S > 0.75), the peak roof acceleration demand is reduced to account for in-plane yielding of the diaphragm.

Out-of-plane Wall Drift Demand: Out-of-plane wall drift demand is determined based on peak ground acceleration (PGA) and wall out-of-plane design strength. Overstrength of out-of-plane walls was incorporated in the SRPE calibration process by modeling out-of-plane wall bending elements with their expected strength properties in OpenSEES. Expected strengths were determined by dividing out the strength reduction factor (ϕ) and scaling the nominal strength to account for expected material properties. The relationship between PGA and out-of-plane wall drift demand is nonlinear. Once yielding begins, the wall's low post-yield stiffness and limited hysteretic energy dissipation cause out-of-plane drift to increase more rapidly with increasing PGA.

Story Drift Ratio: Story drift ratio is predicted from $Sa(T_1)$ and the strength factor, S. Story drift ratio is primarily due to in-plane diaphragm deflection and therefore should not be applied as an in-plane wall demand. Additionally, because gravity columns within RWFD buildings have such high displacement capacity, they can be considered rugged as well. Therefore, story drift ratio is not an important EDP for assessing safety critical damage in RWFD buildings, but may still be critical to limit damage to non-structural in the building. Damage to non-structural components in not explicitly considered in the structural system prequalification assessment procedure.

Residual Story Drift Ratio: Residual story drift ratio is predicted from story drift ratio and yield drift. The probability of residual story drift ratio large enough to result in red tag and/or demolition in RWFD buildings is essentially zero at shaking intensities at or below the DE.

3. RESULTS

The plots below show the $R_{diaph,fr}$ and $I_{p,fr,oop}$ envelope for each performance group variant combination. This design envelope identifies the possible design value combinations where all performance groups satisfy both the max and mean analysis criteria. Results are provided separately for both FRC A/B/C acceptance criteria in Section 3.1 and FRC D acceptance criteria in Section 3.2. Additional figures are provided that illustrate controlling component damage are provided in Section 3.3. Full details on the performance of individual archetypes are provided in the attached supplementary materials.

3.1. FRC A/B/C Analysis Results

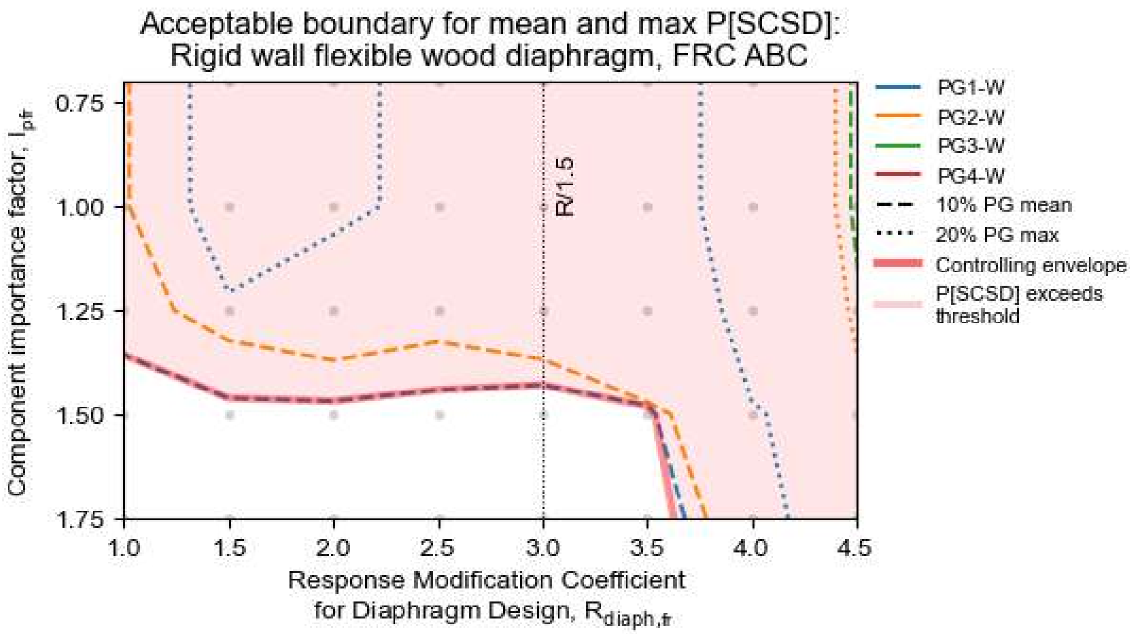

Figure 22 – Combination of $R_{diaph,fr}$ and $I_{p,fr,oop}$ values required to satisfy the FRC A/B structural performance acceptance criteria for each performance group.

3.2. FRC D Analysis Results

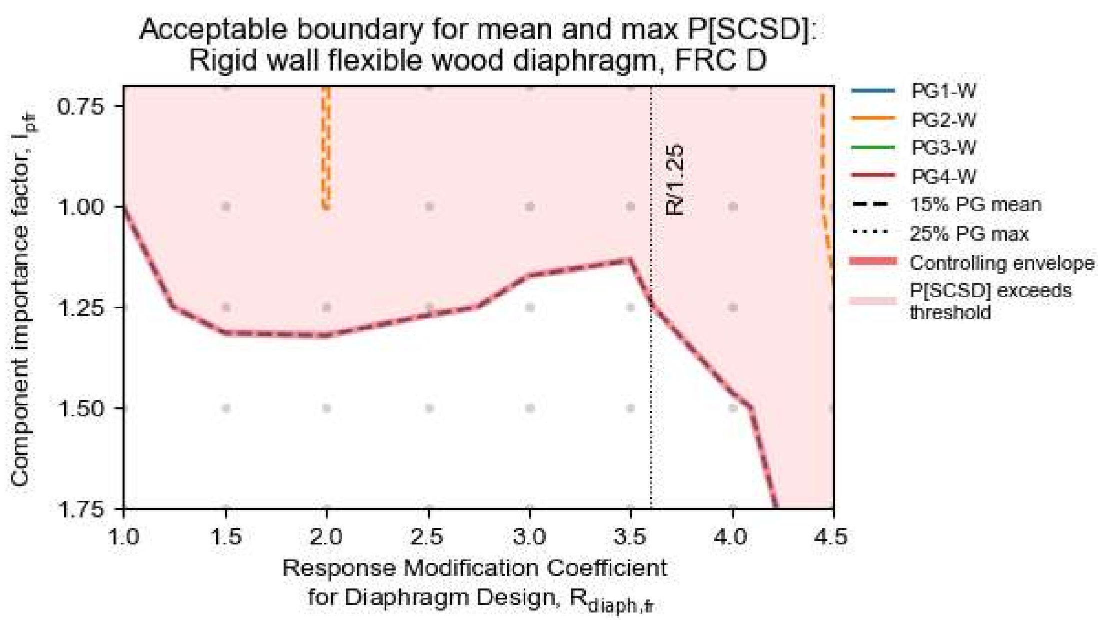

Figure 23 – Combination of $R_{diaph,fr}$ and $I_{p,fr,oop}$ values required to satisfy the FRC D structural performance acceptance criteria for each performance group.

3.3. System Response

Breakdowns of the contributions to SCSD by structural component type are provided in Figure 24 and Figure 25 for the recommended $R_{diaph,fr}$ and $I_{p,fr,oop}$ combinations for FRC A/B/C and D, respectively.

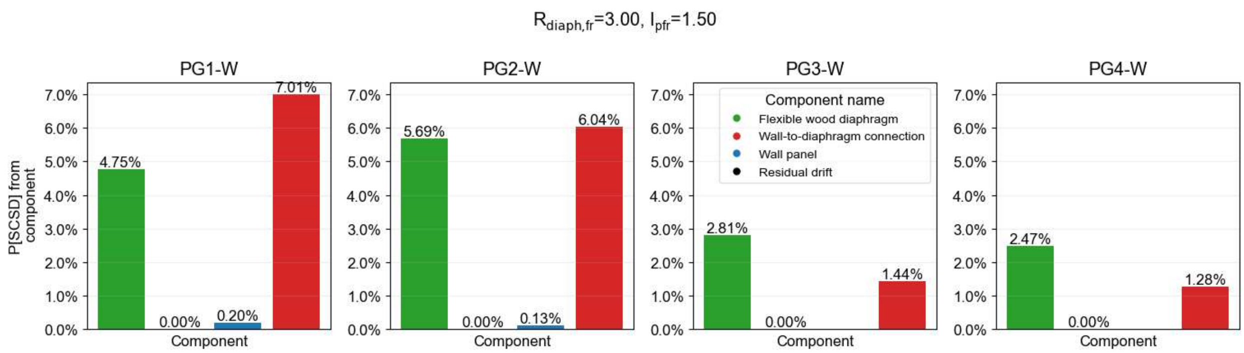

Figure 24 – Component damage contribution to P[SCSD] for wood diaphragm performance groups at the FRC A/B/C recommended R_{fr}=3.0 and $I_{pfr,oop}$ =1.50.

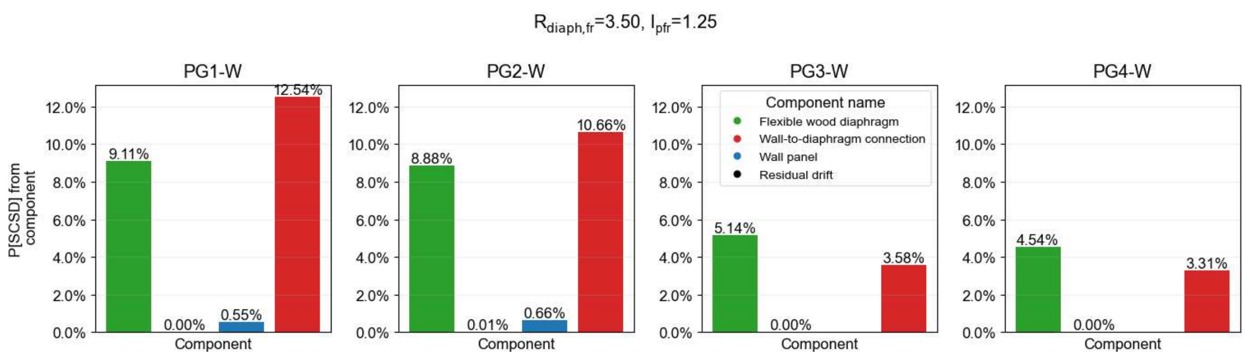

Figure 25 – Component damage contribution to P[SCSD] for wood diaphragm performance groups at the FRC D recommended $R_{diaph,fr}$=3.5 and $I_{pfr,oop}$ =1.25.

3.4. Validation of Peak Floor Acceleration Demand Estimates

The prequalification method documented in the 2026 NEHRP Section A.8.3.6 requires that the peak floor acceleration demands be evaluated for all of the structural system archetype design cases, to ensure that the Section A.10.6 peak floor acceleration adequately reflect the actual peak floor acceleration values observed in the nonlinear response-history analysis results. If the peak floor acceleration demands exceed the acceptable limits of Section A.8.3.6, the recommended $R_{\mu fr}$ value is reduced from the baseline $R_{\mu fr}$ value to adequately adjust the peak floor acceleration demands when using the Section A.10.6 equation. The baseline $R_{\mu fr}$ values are calculated in accordance with Section 13.3.1.2 with the following modifications:

1. R_{fr} and Ω_{0fr} are used in lieu of R and Ω_0
2. The value of Ie is taken as 1.0.
3. The lower limit on $R_{\mu fr}$ of 1.3 in Equation 13.3-6 does not apply.

The recommended R_{ufr} values are determined by checking for compliance with the following two criteria:

1. The ratio of the median peak floor acceleration from analysis averaging across all structural levels to the seismic floor acceleration determined in accordance with Section A.10.7 averaged across all structural levels is computed. The average of this ratio across all archetypes within a performance group shall not exceed 1.0.
2. The ratio of the largest peak floor acceleration from analysis at any level to the largest seismic floor acceleration determined in accordance with Section A.10.7 at any structural level is computed. The average of this ratio across all archetypes within a performance group shall not exceed 1.2.

The Section A.8.3.6 evaluation was completed, resulting in the following $R_{\mu fr}$ requirements:

- $R_{\mu fr}$ = 1.3 is required for FRC A/B/C (based on design using R_{fr} = 3.0 and $\Delta_{a,diaph,fr}$ = 1.25%, $I_{pfr,oop}$ = 1.50), which is larger than the baseline value of 1.25. Therefore, no change required.
- $R_{\mu fr}$ = 1.35 is required for FRC D (based on design using R_{fr} = 3.5 and $\Delta_{a,diaph,fr}$ = 1.75%, $I_{pfr,oop}$ = 1.25), which is slightly smaller than the baseline value of $R_{\mu fr}$ = 1.4.

For RM-RWFD buildings, the design drift limit does not affect the resulting seismic qualification factors because the diaphragm ductility demand is used as a more direct measure of diaphragm damage. Therefore, the story drifts of the archetype models assessed in this study were not explicitly limited to the judgment-threshold. While most of the RM-RWFD archetypes have story drifts below the limit at the recommended $R_{diaph,fr}$ value, the large RM-RWFD archetypes of PG3 and PG4 exceeded the judgment-based limit. However, the accelerations from the PG3 and PG4 archetypes did not control the $R_{\mu fr}$ values presented above. The authors of this study verified that stiffening the diaphragms of the large RM-RWFD archetypes to meet the prescribed drift limit of 1.25% does not impact the $R_{\mu fr}$ values presented above.

4. CONCLUSIONS AND RECOMMENDATIONS

This report documents the quantification of the functional recovery seismic performance factors for the RM-RWFD system in accordance with the proposed Section A.8 procedures of the 2026 National Earthquake Hazards Reduction Program (NEHRP) Provisions. The analysis in this report quantified the design requirements for one-story masonry RWFD with wood diaphragms, and then the recommendations both generalize those results to other diaphragm cases and provide details of the other design considerations beyond the diaphragm.

4.1. Design Strength Requirements for Wood Diaphragms in Masonry RWFD Buildings

The recommended functional recovery seismic performance factors, including the diaphragm functional recovery response modification coefficient, $R_{diaph,fr}$, and the component importance factor used for out-of-plane design forces for walls and wall anchorage, $I_{p,fr,oop}$, for the RM-RWFD system with wood diaphragms are summarized in Table 9. These analyses were run using the 2021 NDS wood diaphragm design strength methods, which has revised the strength estimations in a manner that will add 14% additional strength to wood diaphragms.

As shown in the previous sections, safety-critical structural damage in the RM-RWFD archetypes was primarily driven by a combination of flexible wood diaphragm damage and isolated out-of-plane walls connection failures, with recommendations for $R_{diaph,fr}$ controlling diaphragm damage and recommendations for $I_{p,fr,oop}$ controlling, but $R_{diaph,fr}$ influencing, out-of-plane anchorage failures. Safety-critical structural damage was mostly controlled by the mean criteria for the smaller footprint archetypes assessed in performance group PG1 and PG2. The judgement-based limits for $R_{diaph,fr}$ were based on an R_{diaph} factor of 4.5 from ASCE 7 Section 12.10.4. Ultimately, the judgment-based limits for $R_{diaph,fr}$ controlled the final recommended values. Additionally, the final $\Delta_{a,diaph,fr}$ values were dictated by the judgment-based limits, because the story drift ratio was not a primary predictor of safety-critical structural damage for the RM-RWFD buildings assessed.

Section A.10 of the proposed Appendix A NEHRP provision prescribe anchorage force $I_{p,fr}$ values of 1.75 for FRC A/B, 1.50 for FRC C, and 1.25 for FRC D. Table 9 shows that an $I_{p,fr,oop}$ value of 1.5 for the wall out-of-plane anchorage design dis require to meet the performance objectives for FRC A, B, and C, and 1.25 for FRC D. Therefore, the current prescribed values in Section A.10 are sufficient. While the current ASCE 7 design approach for out-of-plane anchorage is expected to be sufficient for life-safety design, additional strength is required to compensate for additional diaphragm demands resulting from reducing $R_{fr,diaph}$ from the 4.5 to the recommended value of 3.0.

Design and detailing of wood diaphragms are required to be according to AWC SDPWS Section 4.2 for blocked diaphragms. The requirement of blocked diaphragms is to be consistent with the analysis assumptions to ensure that the ductility capacity relied on in this study is similar to what is achievable through design. Current expectation of wood diaphragm ductility behavior, such as backbone capacities in ASCE 41-23, suggest that blocking diaphragms provides additional ductility capacity compared to unblocked diaphragms.

Table 9. Summary of functional recovery seismic performance factors for the RM-RWFD system with wood diaphragms.

	FRC A/B/C			FRC D		
	$R_{diaph,fr}$	**$I_{p,fr,oop}$**	**$\Delta_{a,diaph,fr}$**	**$R_{diaph,fr}$**	**$I_{p,fr,oop}$**	**$\Delta_{a,diaph,fr}$**
Analysis with approx. update to 2021 NDS	3.5	1.5	--	4.0	1.25	--
Judgment-based upper limit	3.0	--	1.25%	3.5	--	1.75%
Recommendation –Wood diaphragms† in Special Reinforced Masonry RWFD Buildings	**3.0**	**1.5**	**1.25%**	**3.5**	**1.25**	**1.75%**

† Design and detailing according to AWC SDPWS Section 4.2 for blocked diaphragms

4.2. Design Strength Requirements for Other Types of Diaphragms in Masonry RWFD Buildings

The detailed analyses in this document focused on wood diaphragms, which have well-developed modeling recommendations. Even so, ASCE 7 allows many diaphragm types to be used for masonry RWFD buildings and differentiated R factors are provided in ASCE 7-22 Sections 12.10.4. Therefore, we propose to generalize the recommendations to also cover other diaphragm cases, as shown in Table 10. For this generalization, we observe that our recommended $R_{diaph,fr}$ value of 3.0 for wood diaphragms is 1.5 times lower than the R_{diaph} = 4.5 values suggested in Section 12.10.4. Therefore, we suggest adopting a R/1.5 for ductile steel conforming to AISI S400, which have the same prescribed R_{diaph} as wood diaphragms. Therefore, both wood and ductile steel diaphragms have the same recommended $R_{diaph,fr}$, consistent with their shared R_{diaph} of 4.5 as specified in ASCE 7-22 Section 12.10.4.

Table 10. Summary of functional recovery seismic performance factors for RM-RWFD systems.

	FRC A/B/C			FRC D		
	$R_{diaph,fr}$	**$I_{p,fr,oop}$**	**$\Delta_{a,diap,fr}$**	**$R_{diaph,fr}$**	**$I_{p,fr,oop}$**	**$\Delta_{a,diaph,fr}$**
Wood Diaphragm†	3.0	1.5	1.25%	3.5	1.25	1.75%
Bare Steel Deck Diaphragm – AISI S400 detailing‡	3.0	1.5	1.25%	3.5	1.25	1.75%

† Design and detailing according to AWC SDPWS Section 4.2 for blocked diaphragms
‡ Diaphragm detailing conforms to the special seismic detailing defined in AISI S400 Section F3

4.3. Design Strength Requirements for the Masonry Walls In-Plane

The design of the walls in-plane where not directly evaluated in these analyses, because they are not the controlling failure mode for typical RWFD buildings. The assumption is that the walls in-plane will be stronger than the diaphragm in-plane, though this has not been directly verified. A parallel study is underway to determine the design strength requirements for the masonry structural walls, and we proposed that the results of that study will be used as the design requirement for the in-plane shear design of the masonry walls. This would essentially allow the failure mode to be in either the diaphragm or the wall, with a design R_{fr} factor appropriate to each failure mode. Alternative approaches would be to design the masonry walls in-plane using the same R_{fr} value as the diaphragm, or requiring a capacity check to ensure that the walls are stronger than the diaphragm, but these seem unnecessary, given that R_{fr} values for masonry walls will be developed shortly (and will be submitted as part of the January 2026 PUC proposal package).

4.4. Design Strength Requirements for the Masonry Walls Out-of-Plane

The full masonry RWFD analyses documented in this report includes damage assessment looking at the wall out-of-plane bending behavior. It shows that the wall out-of-plane bending is not a controlling damage mode for functional recovery, when designed per typical ASCE 7 Section 12.11.1 procedures. Therefore, the results in this report support not requiring any addition design strength for wall out-of-plane bending.

4.5. Use of the Various ASCE 7 Design Methods for RWFD Buildings

ASCE 7-22 currently has three design methods that can be used for designing RWFD buildings (Sections 12.10.1, 12.10.3, and 12.10.4), each resulting in potentially different building designs. These recommendations are intended for use with both the Section 12.10.1 and Section 12.10.4 methods.

In the Section 12.10.1 design approach, the diaphragm is designed with the same R factor as the LFRS. These analysis results show that Section 12.10.1 can be used, but with $R_{diaph,fr}$ values that may vary with diaphragm type.

This study does not consider the Section 12.10.3 design approach and has not confirmed that these recommended design values can be used with the Section 12.10.3 approach.

For the Section 12.10.4 design approach, diaphragm design forces can be smaller than with the 12.10.1 method due to the fundamental period being in the constant velocity portion of the design spectrum. However, diaphragm behavior is enhanced by requiring additional strength near collectors. Additional analyses were performed by re-proportioning all of the archetypes using the 12.10.4 design procedure, and these confirmed that the recommended design values still meet the performance targets when the 12.10.4 diaphragm design procedure is used.

SUPPLEMENTARY MATERIAL

Two supplementary files are attached to this Prequalification Report that provide additional detailed information on the structural response and ATC 138 outcomes from individual archetype models and performance groups. The general description of the content contained in each file is provided below to assist with navigation and comprehension of detailed results.

- **Analysis Report Tables** *SupplementalData_AnalysisReportTables_RWFD_ v1_4e.xlsx*
    - Contains detailed analysis outcomes for each archetype model assessed, including results for FRC A/B/C and FRC D.
    - "Summary" tab provides a summary of the controlling design values and other response metrics for each archetype
    - "All Runs" tab provides response and performance outcomes for all combinations of model runs for each archetype.
- **Archetype Performance Plots** *SupplementalData_ArcehtypePerformancePlotsAppendix_ RWFD_v1_4e.pdf*
    - Provides visualizations of analysis outcomes similar to the figures in the report, but for individual archetype models.
    - Provide peak drift and peak floor acceleration response profiles for each archetype model.

REFERENCES

ABK. (1981). "Methodology for Mitigation of Seismic Hazards in Existing Unreinforced Masonry Buildings: Diaphragm Testing," Agbabian-Barnes-Kariotis Joint Venture, *Topical Report No. ABK-03*, El Segundo, California.

Adham, A.A., Avanessian, V., Traina, I. (1988). "Out-of-Plane Dynamic Testing of Concrete Masonry Walls," *Report No.3.2.(b1)*, conducted at Agbabian Associates, El Segundo, California, for the University of Southern California, Department of Civil Engineering, University Park, Los Angeles, California.

ACI-SEAOSC. (1982). "Test Report on Slender Walls," By the ACI-SEAOSC Task Committee on Slender Walls, Structural Engineers Association of Southern California, Whittier, CA.

AF&PA, 2005b, Special Design Provisions for Wind and Seismic, ANSI/AF&PA SDPWS-2005, American Forest & Paper Products Association, Washington, D.C.

AISC. (2022). "Seismic Provisions for Evaluation and Retrofit of Existing Structural Steel Buildings," *ANSI/AISC 342-22*, American Institute of Steel Construction, Chicago, IL.

AISI. (2020a). "North American standard for the design of profiled steel diaphragm panels," *ANSI/AISI S310-20*, American Iron and Steel Institute, Washington, DC.

AISI. (2020b). "North American standard for seismic design of cold-formed steel structural systems," *ANSI/AISI S400-20*, American Iron and Steel Institute, Washington, DC.

Almeter, E., Wade, K.F., Haselton, C.B., Saxey, B. (2018). "Rapid Risk Assessment of Buckling Restrained Braced Frames, With Focus on Residual Drifts," *Proceedings of the 11th U.S. National Conference on Earthquake Engineering* (11NCEE), Los Angeles, CA.

ASCE. (2006). "Seismic Evaluation and Retrofit of Existing Buildings," *ASCE/SEI 41-06*, American Society of Civil Engineers, Reston, VA.

ASCE. (2022). "Minimum Design Loads and Associated Criteria for Buildings and Other Structures," *ASCE/SEI 7-22*, American Society of Civil Engineers, Reston, VA.

ASCE. (2023). "Seismic Evaluation and Retrofit of Existing Buildings," *ASCE/SEI 41-23*, American Society of Civil Engineers, Reston, VA.

ATC. (2021). "Seismic Performance Assessment of Buildings: Volume 8 – Methodology for Assessment of Functional Recovery Time, *ATC-138-3*, Preliminary report for FEMA P-58-8, Prepared by the Applied Technology Council for the Federal Emergency Management Agency, Washington, DC.

AWC. (2021). "Special Design Provisions for Wind and Seismic," *ANSI/AWS SDPWS-2021*, American Wood Council, Leesburg, Virginia.

Blowes, K., Molina-Hutt, C., Zimmerman, R., Cook, D.T., Almeter, E., Haselton, C.B. (2025). "Limiting Safety-Critical Structural Damage in Recovery-Based Seismic Design Provisions," *Earthquake Spectra* (in press).

Carter, J.W., Hawkins, N.M., Wood, S.L. (1993). "Seismic Response of Tilt-Up Construction," *Civil Engineering Studies SRS-581,* University of Illinois, Urbana, IL.

Cohen, G.L., Klingner, R.E., Hayes, J.R., Sweeney, S. C. (2004). "Seismic evaluation of low-rise reinforced masonry buildings with flexible diaphragms. I. Seismic and quasi-static testing." *Earthquake Spectra*, **20**(3): 779–801.

Cook, D., Wade, K., Haselton, C., Baker, J. W., DeBock, D. J. (2018). A structural response prediction engine to support advanced seismic risk assessment. In Eleventh US national conference on earthquake engineering, Los Angeles, CA.

Countryman, D. (1952). "Lateral Tests of Plywood Sheathed Diaphragms," *Laboratory Report 55*, Douglas Fir Plywood Association.

Countryman, D. (1955). "Horizontal Plywood Diaphragm Tests," *Laboratory Report 63*, Douglas Fir Plywood Association.

DeBock, D., Manousakis, I.V., Deierlein, G.G., Zsarnóczay, A. (2024). "Updated Model and Criteria for Residual Drift," *FEMA P-58/BD-3.7.26*, Background documentation for the ATC-138/FEMA P-58 Project, Submitted to the Applied Technology Council, Prepared for the Federal Emergency Management Agency, Washington, DC.

Eatherton, M.R., O'Brien, P.E. Samuel Easterling, W. (2020). "Examination of ductility and seismic diaphragm design force-reduction factors for steel deck and composite diaphragms," *Journal of Structural Engineering*, **146**(11): 04020231.

FEMA. (1997). "NEHRP Commentary on the Guidelines for the Seismic Rehabilitation of Buildings," *FEMA-274*, Prepared by the Applied Technology Council for the Building Seismic Safety Commission and the Federal Emergency Management Agency, Washington, DC.

FEMA. (1999). "Evaluation of Earthquake Damaged Concrete and Masonry Wall Buildings – Technical Resources," *FEMA 307*, Prepared by the Applied Technology Council for the Federal Emergency Management Agency, Washington, DC.

FEMA. (2009). "Quantification of Building Seismic Performance Factors," *FEMA P695*, Prepared by the Applied Technology Council for the Federal Emergency Management Agency, Washington, DC.

FEMA. (2015). "Seismic Design of Rigid Wall-Flexible Diaphragm Buildings," *FEMA P-1026*, 1st Edition, Prepared by the Applied Technology Council for the Federal Emergency Management Agency, Washington, DC.

FEMA. (2018a). "Seismic Performance Assessment of Buildings: Volume 1 – Methodology," *FEMA P-58-1*, 2nd Edition, Prepared by the Applied Technology Council for the Federal Emergency Management Agency, Washington, DC.

FEMA. (2018b). "Seismic Performance Assessment of Buildings: Volume 2 – Implementation Guide," *FEMA P-58-2*, 2nd Edition, Prepared by the Applied Technology Council for the Federal Emergency Management Agency, Washington, DC.

FEMA. (2021). "Seismic Design of Rigid Wall-Flexible Diaphragm Buildings," *FEMA P-1026*, 2nd Edition, Prepared by the Applied Technology Council for the Federal Emergency Management Agency, Washington, DC.

Haselton Baker Risk Group (2025). Seismic Performance Prediction Program (SP3).

Koliou, M. (2014). "Seismic analysis and design of rigid wall-flexible diaphragm roof structures," *PhD Dissertation*, University at Buffalo – State University of New York Buffalo, NY.

Koliou, M., Filiatrault, A., Kelly, D.J., Lawson, J. (2015). "Distributed Yielding Concept for Improved Seismic Collapse Performance of Rigid Wall-Flexible Diaphragm Buildings," *Journal of Structural Engineering*, **142**(2): 04015137.

Koliou, M., Filiatrault, A., Kelly, D.J., Lawson, J. (2016a). "Buildings with Rigid Walls and Flexible Roof Diaphragms. I: Evaluation of Current U.S. Seismic Provisions," *Journal of Structural Engineering*, **142**(3): 04015166.

Koliou, M., van de Lindt, J.W., Filiatrault, A. (2016b). "Evaluation of an alternative seismic design approach for rigid wall flexible wood roof diaphragm buildings through probabilistic loss estimation and disaggregation," *Engineering Structures*, **127**(15): 31-39.

Koliou, M., Lawson, J., Filiatrault, A., Kelly, D.J. (2017a). "Evaluation of out-of-plane wall anchorage force provisions in buildings with rigid walls and flexible roof diaphragms," *Earthquake Spectra*, **33**(1): 1-23.

Koliou, M., Masoomi, H., van de Lindt, J.W. (2017b). "Performance Assessment of Tilt-Up Big-Box Buildings Subjected to Extreme Hazards: Tornadoes and Earthquakes," *Journal of Performance of Constructed Facilities*, **31**(5): 04017060.

Koliou, M., Filiatrault, A. (2017). "Development of Wood and Steel Diaphragm Hysteretic Connector Database for Performance-Based Earthquake Engineering," *Bulletin of Earthquake Engineering*, **15**(10): 4319-4347.

Lawson, J.W. (2007). "Thinking Outside the Box: New approaches to very large flexible diaphragms," *SEAOC 2007 Convention Proceedings*, Structural Engineers Association of California.

Lawson, J.W. (2008). "Tilt-up Buildings," *The SEAOC Bluebook: Seismic Design Recommendations*, Structural Engineers Association of California.

Lawson, J.W., Lai, J. (2010). "Concrete Slender Wall Design – Back to the Future," *Proceedings of the 2010 SEAOC Convention*, Indian Wells, CA.

Lawson, J. (2013). "Seismic Design of Timber Panelized Roof Structures," *WoodWorks*, Wood Products Council, Washington, D.C.

Lawson. J.W. (2017). "Discussions of fragility function adjustments for out-of-plane wall and connection behavior in tilt-up buildings," *Personal Communication*, November 2017, to Haselton Baker Risk Group, John Lawson, Professor, California Polytechnic University, San Luis Obispo, CA.

Lawson, J., Koliou, M. (2020). "Evaluating second-order effects in rigid wall-flexible diaphragm roof diaphragm buildings," *Earthquake Spectra*, **36**(4): 1864-1885.

McKenna, F., Scott, M.H., Fenves, G.L. (2010). "Nonlinear Finite-Element Analysis Software Architecture using Object Composition," *Journal of Computing in Civil Engineering*, **24**(1): 95-107.

Miranda, E. (1999). "Approximate seismic lateral deformation demands in multistory buildings," *Journal of Structural Engineering*, **125**(4): 417-425.

Miranda, E., Reyes, C.J. (2002). "Approximate lateral drift demands in multistory buildings with nonuniform stiffness," *Journal of Structural Engineering*, **128**(7): 840-849.

O'Brien, P., Eatherton, M.R., Easterling, W.S., Schafer, B.W., Hajjar, J.F. (2017). "Steel deck diaphragm test database v1.0," *CFSRC R-2017-03*, Cold-Formed Steel Research Consortium, Johns Hopkins University, Baltimore, MD.

SDI. (2015). "Diaphragm Design Manual," 4th Edition, *DDM04*, Steel Deck Institute, Glenshaw, Pennsylvania.

Schafer, B.W., Smith, B.H., Torabian, S., Meimand, V., Eatherton, M.R. (2018). "Modeling and performance of thin-walled steel deck in roof diaphragms under seismic demands," *Proceedings of the International Conference on Thin-walled Structures*, Lisbon, Portugal.

Schafer, B.W. (2019). "Research on the Seismic Performance of Rigid Wall Flexible Diaphragm Buildings with Bare Steel Deck Diaphragms," *CFSRC R-2019-02*, Cold-Formed Steel Research Consortium, John Hopkins University, Baltimore, Maryland.

SEAONC (2001). "Guidelines for Seismic Evaluation and Rehabilitation of Tilt-up Buildings and Other Rigid Wall/Flexible Diaphragm Structures," Structural Engineers Association of Northern California: San Francisco, CA.

Tissell, J.R., (1967). "1966 Horizontal Plywood Diaphragm Tests," *APA Laboratory Report 106*, American Plywood Association, Tacoma, WA.

Tissell, J.R., Elliott, J.R. (2001). "Plywood Diaphragms," *APA Research Report 138*, Revised July 2001, APA – The Engineered Wood Association, Tacoma, WA.

Torabian, S., Schafer, B.W. (2021). "Cyclic experiments on sidelap and structural connectors in steel deck diaphragms," *Journal of Structural Engineering*, **147**(4): 04021028.

Vamvatsikos, D., Cornell, C.A. (2002). "Incremental Dynamic Analysis," *Earthquake Engineering and Structural Dynamics*, **31**(3): 491-514.

Vouvakis Manousakis I., Zsarnoczay A., Konstantinidis D., (2024), "Robust Residual Drift Estimation for Seismic Performance Assessment based on High-Fidelity Response Simulation of Steel Frames," (manuscript in preparation).

Wade, K.F., DeBock, D.J., Lawson, J.W., Koliou, M., Cook, D.T., Haselton, C.B. (2018). "Seismic Risk Assessment of Tilt-Up Buildings Using the FEMA P-58 Method," *Proceedings of the 11th U.S. National Conference on Earthquake Engineering* (11NCEE), Los Angeles, CA.

Wei, G., Eatherton, M.R., Schafer, B.W. (2019). "Development of Steel Deck Diaphragm Seismic Design Provisions for ASCE 41/AISC 342, *CFSRC R-2019-01*, Cold-Formed Steel Research Consortium, John Hopkins University, Baltimore, Maryland.

Whitney, R., Agrawal, A.K. (2015). "Seismic performance of flexible timber diaphragms: Damping, force-displacement and natural period," *Engineering Structures*, **101**: 583-590.